Author(s) and affiliations: Colm Clancy, Rónán Darcy, Emily Gleeson, Alan Hally, Eoin Whelan

Research, Environment and Applications Division, Met Éireann.

Met Éireann
Technical Note No. 66

HARMONIE-AROME 40h1.1 Upgrade

Colm Clancy, Rónán Darcy, Emily Gleeson, Alan Hally, Eoin Whelan

Met Éireann
2018

Disclaimer

ISSN 1393-905X

Title: HARMONIE-AROME 40h1.1 Upgrade
Authors: Colm Clancy, Rónán Darcy, Emily Gleeson, Alan Hally, Eoin Whelan

Corresponding author: Colm Clancy (colm.clancy@met.ie)

Abstract

The operational Numerical Weather Prediction suite at Met Éireann was upgraded on the 1st of May 2018. Cycle 40h1.1 of the HARMONIE-AROME model was introduced, replacing the previous operational cycle 37h1.1. The major changes with the upgrade were an enlarged model domain and the introduction of 3D-Var data assimilation with 3-hour cycling.

In preparation for this upgrade, extensive testing and validation of cycle 40h1.1 was carried out. Forecasts of representative periods were compared with the operational model. Initial tests with the default set-up revealed a significant cold bias in near-surface temperature forecasts. To reduce this bias, a number of modifications to the cycle 40h1.1 configuration were made. Changes to the turbulence scheme and the surface analysis improved the verification scores for 2 m temperature. These, however, had a negative impact on the accuracy of the near-surface wind-speed forecasts. This was addressed by tuning the surface drag effects. Pre-operational testing with month-long experiments produced an overall neutral or positive impact on the verification scores, when compared with the operational cycle 37h1.1. In addition, analysis of a number of case studies showed no particular disadvantages to the new set-up.

The new operational cycle 40h1.1 was initially run in parallel with cycle 37h1.1. Performance scores for May 2018 were broadly neutral, showing both slight improvements in some fields, and some slightly negative effects in others.

Contents

1 Introduction

The main limited area model currently in operational use for Numerical Weather Prediction (NWP) at Met Éireann is the nonhydrostatic mesoscale HARMONIE-AROME configuration of the shared ALADIN-HIRLAM NWP system, hereafter referred to as HARMONIE-AROME. A full model description may be found in Bengtsson et al. (2017); details of the configuration used by the ALADIN consortium are given in Termonia et al. (2018). HARMONIE-AROME was first made operational at Met Éireann on the 11^{th} of July 2011 using cycle 36h1.3 and cycle 37h1.1 was introduced on the 31^{st} of January 2013.

On the 1^{st} of May 2018, the NWP suite was upgraded and cycle 40h1.1 was used for the 1200 UTC forecast. This Technical Note describes this upgrade and details the local changes made to the model configuration, along with the extensive testing that was carried out by the NWP staff in the Research, Environment and Applications (REA) division throughout 2017 and early 2018.

2 Cycle 40h1.1 configuration

2.1 40h1.1 details

HARMONIE-AROME cycle 40h1.1 was released on September 23rd 2016. The cycle 40h1.1 release notes (HIRLAM, 2016) provide a summary of cycle 40h1.1 scientific and technical changes compared with the previous cycle, cycle 38h1.2.

2.2 Model grid definition

In Table 1, we provide details of the HARMONIE-AROME domains used at Met Éireann. As part of the upgrade to cycle 40h1.1, the size of operational domain was increased. Fig. 1 shows both the old and the new, larger domain. While there is no change in the horizontal or vertical spatial resolutions, the time-step has been increased from 60 s to 75 s. This new value is the default for cycle 40h1.1 (Bengtsson et al., 2017).

	36h1.3	**37h1.1**	**40h1.1**
Horizontal	540×500	540×500	1000×900
Grid spacing	2.5 km	2.5 km	2.5 km
Vertical	60	65	65
Model top	10 hPa	10 hPa	10 hPa
Time-step	60 s	60 s	75 s

Table 1: Details of old and new operational grids.

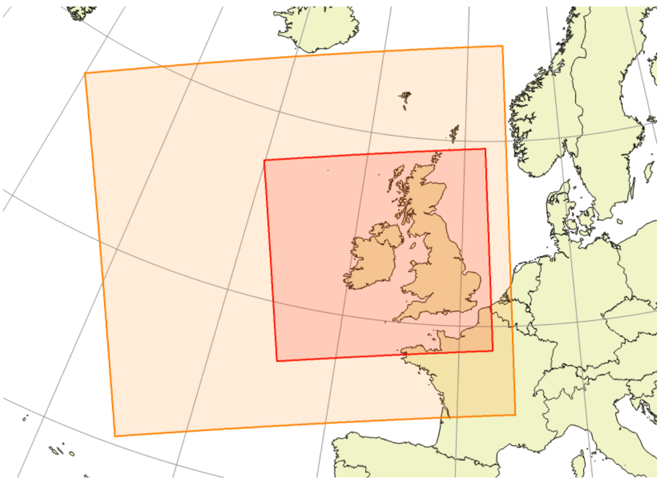

Figure 1: Current operational (red) and new enlarged domain (orange)

3 Initial model assessment

The initial tests on cycle 40h1.1 began in early 2017. A number of representative cases were chosen for testing the performance against the operational cycle 37h1.1 model in month-long simulations. These included typical Irish wet and windy winter conditions in December 2015, the unusually cold and snowy December 2010, and hot summer conditions in June 2014.

In these first tests cycle 40h1.1 was run without 3D-Var data assimilation, and using the same, smaller, domain of the operational model to provide a fair comparison with the operational forecasts. Default settings and parameter values were used; essentially, we compared cycle 40h1.1 default settings against the existing operational model, hereafter referred to as oper37.

NWP model accuracy is verified by comparing forecasts at point locations with observations at synoptic stations using a number of metrics. Within the HIRLAM consortium, a software package known as "monitor" has been developed to carry out this analysis and produce statistical and graphical output. This is used extensively throughout this Technical Note, in particular to examine and compare the root-mean-square error (RMSE) and bias of HARMONIE-AROME forecasts.

In Fig. 2, verification results are shown for the December 2015 simulations. On the top row are scores for the 10 m wind-speed, while below are those for 2 m temperature. The verification is separated into forecasts commencing at 0000 UTC (left) and 1200 UTC (right).

These verification scores are typical of the results found in this initial test phase. Looking first at the wind (Fig. 2a and 2b), we see a noticeable improvement in 40h1.1 (green curves) in both RMSE and bias when compared with oper37 (red). This performance holds throughout the forecast and both during the day and at night.

Unfortunately, the results are less promising for 2 m temperature (Fig. 2c and 2d). In particular, a significant cold bias is visible in 40h1.1, with a magnitude of up to 1 degree. Examining the bias pattern of the forecasts from different times, it is clear that the problem is worse during the night.

This cold bias was observed in each of the different test periods, but was at its worst for the wet conditions of December 2015. In general, the magnitude of the bias was between 0.5 and 1 degree. Numerous experiments with different radiation options, a larger domain, and various 3D-Var set-ups failed to improve this.

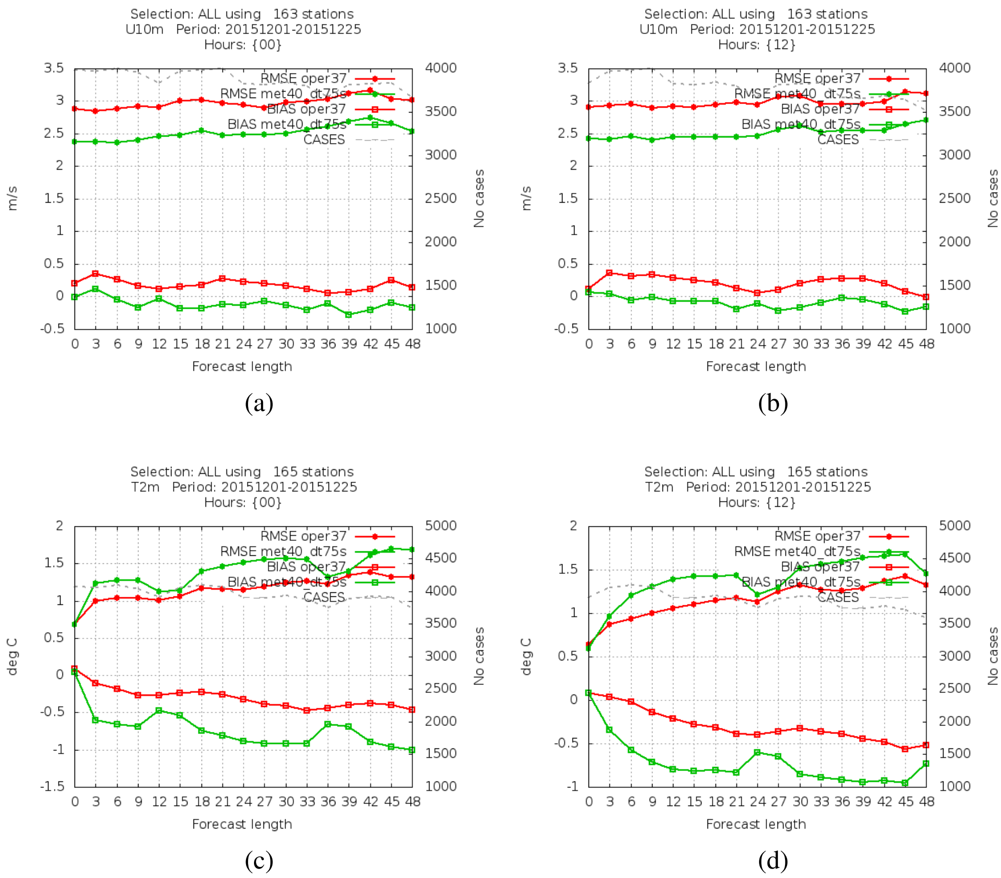

Figure 2: Point verification for December 2015 forecasts during the initial test phase, comparing the operational cycle 37h1.1 (oper37, red) and default cycle 40h1.1 (met40_dt75, green) for the following: 10 m wind-speed from (a) 0000 UTC and (b) 1200 UTC forecasts, and 2 m temperature from (c) 0000 UTC and (d) 1200 UTC forecasts.

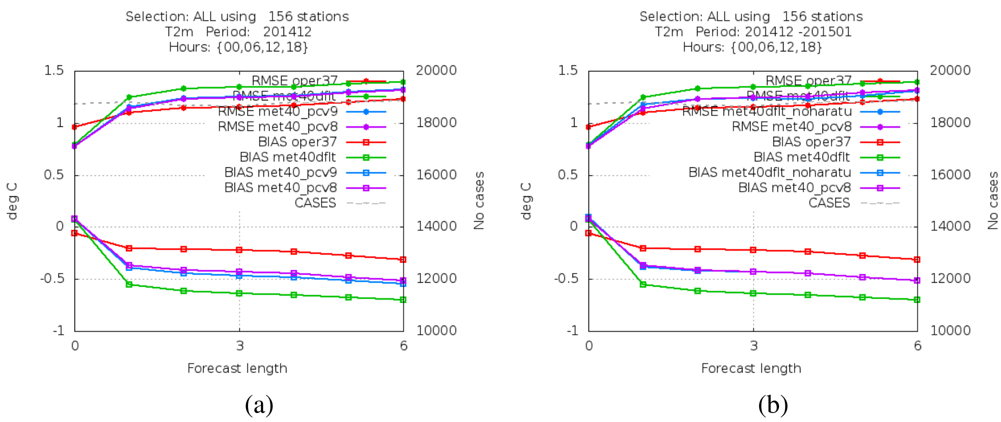

Figure 3: Point verification of 2 m temperature for December 2014 forecasts during the initial test phase, comparing the operational cycle 37h1.1 (oper37, red) and default cycle 40h1.1 (met40dflt, green) with other cycle 40h1.1 experiments as follows: (a) PCV = 9×10^{-6} (met40_pcv9, blue) and 8×10^{-6} (met40_pcv8, magenta); (b) HARATU=no (met40dflt_noharatu, blue), HARATU=yes and PCV = 8×10^{-6} (met40_pcv8, magenta)

4 Forecast model settings

A second phase of testing begin in early 2018, with the aim of addressing the temperature bias described above, and settling on a suitable operational configuration for the HARMONIE-AROME forecast model. Following discussions with HIRLAM and Météo-France researchers, it was suggested that forecast model sensitivity to PCV settings, vegetation heat capacity in SURFEX surface model, be evaluated. By default this has a general value of 2×10^{-5}, and 1×10^{-5} for certain tree types. We carried out experiments with lower values of 8×10^{-6} and 9×10^{-6}. Results for a series of short, 6-hour forecasts throughout December 2014 are shown in Fig. 3a, in which an improvement in 2 m temperature bias is visible. As part of the tests with physics options, the HARATU turbulence scheme was switched off. In the verification shown in Fig. 3b, we see that this has a beneficial effect on the temperature bias, of similar magnitude to that from the PCV changes.

4.1 Atmospheric model settings

Two short test periods were chosen to begin with. From the 1st to 3rd of June 2016, the conditions over Ireland were almost entirely cloud-free with very light winds (Fig. 4). Such a period allows us to rule out cloud effects when interpreting results. The second period was the first week in December 2015. As described in the previous section, the weather was the typically wet and windy Irish winter. The periods represent dry and wet soil conditions, respectively, and could be used to highlight differences due to vegetation or other surface modelling effects. A number of physics options were identified for study: the HARATU turbulence scheme (which had earlier been shown to improve the bias), OCND2 cloud physics and radiation updates included in cycle 40h1.1.

In Fig. 5 we show 2 m temperature verification of 1200 UTC forecasts for the clear-sky June case for various experiments with these physics options. In this situation, the operational cycle 37h1.1 (oper37, in red) has a slight cold bias during the day and slight warm bias at night. The default cycle 40h1.1 (40dflt, green) shows a cold bias during the night.

Of the remaining experiments, those in Fig. 5a have OCND2 switched off, while those in Fig. 5b have HARATU switched off. In Fig. 5a, we see little effect in simply switching off OCND2 and leaving everything else set to defaults (No_OCND2, dark blue). This is to be expected in this cloud-free case. Looking at the rest of the experiments in both Fig. 5a and Fig. 5b, we see that setting HARATU=no has some effect (No_HARATU, dark blue in Fig. 5b), whereas any additional modifications do not change the results significantly.

As stated earlier, this is a useful case to look at a cloud-free situation. However it must be noted that the time period is short (3 days) and, in addition, the verification in Fig. 5 was carried out for synoptic stations on the island of Ireland only, given that there was cloud-cover over the rest of the domain at this time (Fig. 4). Thus, the number of data points used is too small to draw general conclusions. Nevertheless we once again see an improvement in temperature bias when HARATU is off.

Temperature verification scores for the second test period, the wet and windy December 2015, are shown in Fig. 6. The experiment configurations are the same as for those in Fig. 5, but we now consider all stations in the domain to get slightly more robust statistics. Looking first at Fig. 6a, we see again that simply moving from default cycle 40h1.1 (green) to having no OCND2 does not greatly improve the temperature scores. However, there is a noticeable improvement in both RMSE and bias when we look at any of the experiments without HARATU in Figs. 6a and 6b.

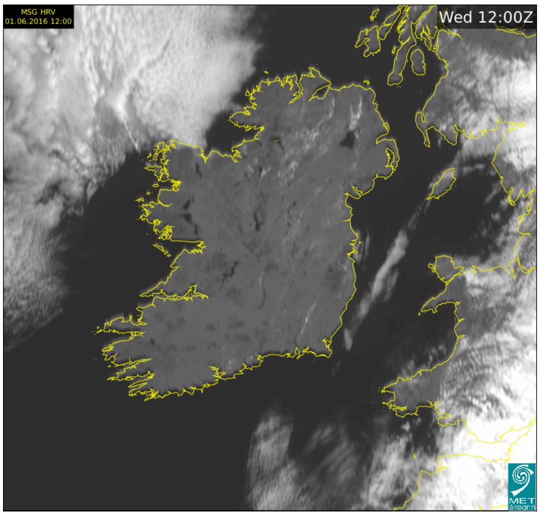

Figure 4: Clear skies over Ireland at 1200 UTC, 1st of June 2016

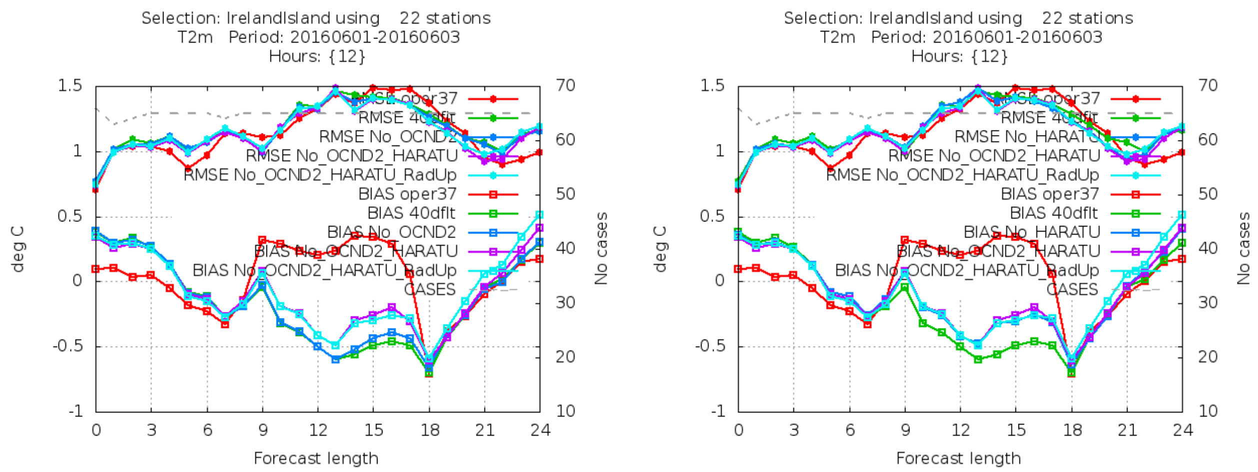

(a) (b)

Figure 5: Point verification of 2 m temperature for stations on the island of Ireland at the beginning of June 2016. Both plots show the operational cycle 37h1.1 (oper37, red) and default cycle 40h1.1 (40dflt, green). (a) Experiments with no OCND2: cycle 40h1.1 with just no OCND2 (No_OCND2, blue); no OCND2 and no HARATU (No_OCND2_HARATU, magenta); no OCND2, no HARATU and no radiation updates (No_OCND2_HARATU_RadUp, cyan). (b) Experiments with no HARATU: cycle 40h1.1 with just no HARATU (No_HARATU, blue); no OCND2 and no HARATU (No_OCND2_HARATU, magenta, as in (a)); no OCND2, no HARATU and no radiation updates (No_OCND2_HARATU_RadUp, cyan, as in (a).

4.2 Surface model settings

As discussed earlier, in the early testing phase the value of PCV, the vegetation heat capacity parameter in SURFEX, was found to have some beneficial effect on the temperature bias. Previously we had reduced the general parameter value from its default 1×10^{-5}. In Figs. 7a and 7b we consider the two test periods with both smaller (8×10^{-8}) and larger (1.2×10^{-5}) values. In both cases, the changes can be seen to warm the model, regardless of whether an increase or decrease. However, it is unclear as to which is better: in the clear, dry case (Fig. 7a), the lower value (blue) leads to severely

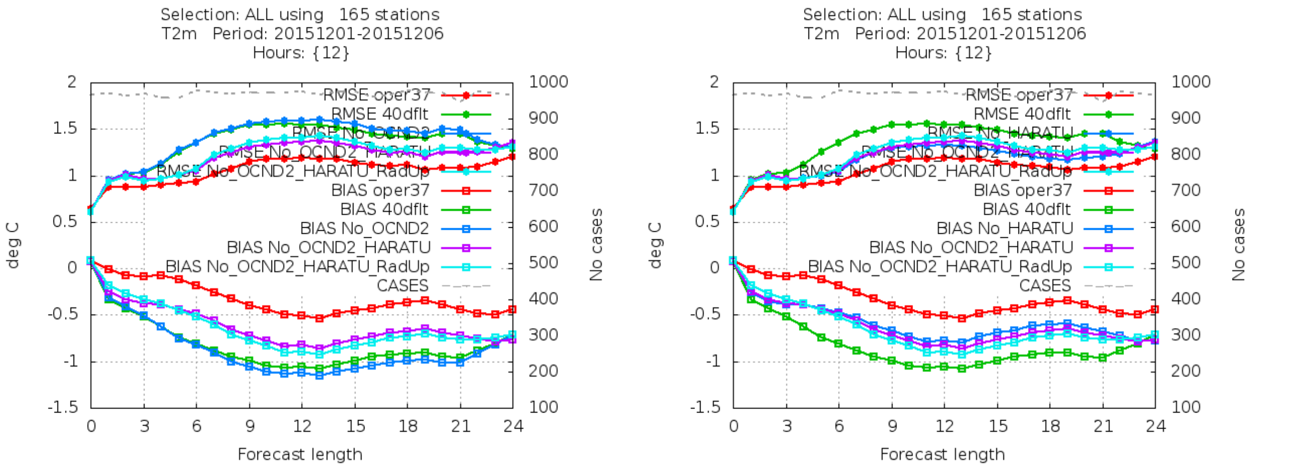

(a) (b)

Figure 6: Point verification of 2 m temperature for all stations for the first week of December 2015. Both plots show the operational cycle 37h1.1 (oper37, red) and default cycle 40h1.1 (40dflt, green). (a) Experiments with no OCND2: cycle 40h1.1 with just no OCND2 (No_OCND2, blue); no OCND2 and no HARATU (No_OCND2_HARATU, magenta); no OCND2, no HARATU and no radiation updates (No_OCND2_HARATU_RadUp, cyan). (b) Experiments with no HARATU: cycle 40h1.1 with just no HARATU (No_HARATU, blue); no OCND2 and no HARATU (No_OCND2_HARATU, magenta, as in (a)); no OCND2, no HARATU and no radiation updates (No_OCND2_HARATU_RadUp, cyan, as in (a).

inaccurate results at night-time, whereas in the wet December case (Fig. 7b, it is the more accurate. Due to this conflicting evidence, it was decided to leave PCV values at the default values.

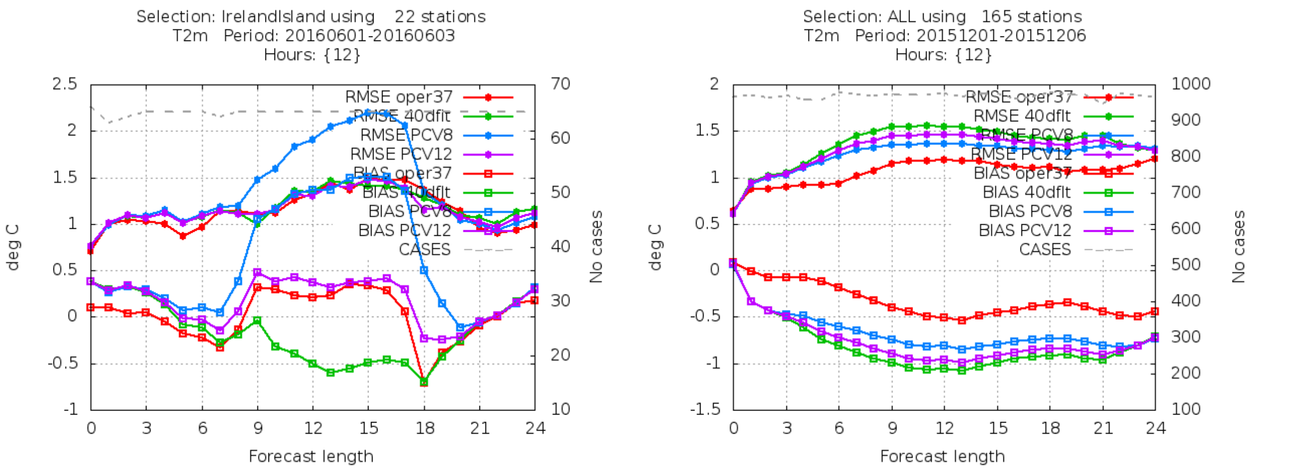

(a) (b)

Figure 7: Point verification of 2 m temperature for various experiments with different PCV values. All have the operational cycle 37h1.1 (oper37, red) and default cycle 40h1.1 (40dflt, green). (a) Clear case, June 2016: PCV = 8×10^{-6} (PCV8, blue); PCV = 1.2×10^{-5} (PCV12, magenta). (b) Wet case, December 2015, as in (a): PCV = 8×10^{-6} (PCV8, blue); PCV = 1.2×10^{-5} (PCV12, magenta).

The default surface physiography database in cycle 40h1.1 is ECOCLIMAP Version 2.2. A further set of experiments were launched to check whether this was a source of error for our temperature forecasts. In Fig. 8 we compare with forecasts run with Version 1.5 for the wet December 2015 week. It is clear that this has little effect on its own (compare the magenta with the 40dflt, in green), and that the effect of the switching off of HARATU still dominates.

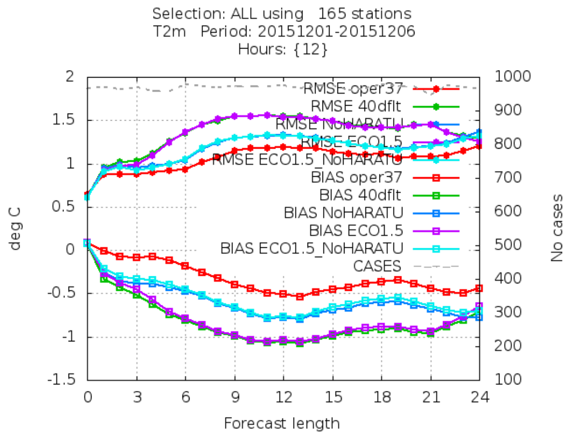

Figure 8: Point verification of 2 m temperature for various experiments for the wet December 2015 case with different versions of the ECOCLIMAP database. Shown are the operational cycle 37h1.1 (oper37, red) and default cycle 40h1.1 (40dflt, green), along with: HARATU=no, default Version 2.2 (NoHARATU, blue); default, with Version 1.5 (ECO1.5, magenta); HARATU=no, Version 1.5 (ECO1.5_NoHARATU, cyan).

One further change, in the SURFEX data assimilation, was suggested. The parameter ZTINER is used in the calculation of the temperature increments in the surface analysis. Following correspondence with HIRLAM colleagues, the value of this was fixed at 2.0 (similar to previous cycles) rather than a derived value. Results for the wet December 2015 are shown in Fig. 9a, where the benefit is obvious, particularly when HARATU is off (magenta). Comparing this with cases where just HARATU is off (for example, the blue curve in Fig. 6b), we see that the ZTINER change adds extra skill to the forecasts.

4.3 Near-surface winds

The results from experiments described above, leading to the results shown in Fig. 9a, suggest an operational cycle 40h1.1 configuration in which HARATU=no and ZTINER=2.0, hereafter denoted NHZ2. Model changes to correct 2 m temperature biases produced 10 m wind-speeds verification statistics shown in Fig.9b. The NHZ2 (magenta), optimal in terms of temperature (Fig. 9a), now shows a degraded wind score when compared with the default cycle 40h1.1 (green), although it should be noted that the RMSE results are still superior to the operational 37h1.1 (red). From the other experiments in (Fig. 9a), it is apparent that the HARATU turbulence scheme improves both the RMSE and bias in 10 m wind-speed when compared with cycle 37h1.1. Turning it off to improve temperatures leads to a positive bias in wind-speed, which needs to be addressed.

To deal with this positive bias, we investigated surface drag effects from three sources. First the XCDRAG parameter, which controls the canopy drag in SURFEX. The default value in cycle 40h1.1 is 0.01. In the operational cycle 37h1.1, a higher value of 0.05 was in use and so this was tested. Next, it had been recommended by HIRLAM colleagues to investigate the leaf-area index (LAI). The resulting drag from LAI over grassland was increased in SURFEX. Finally, an orographic roughness

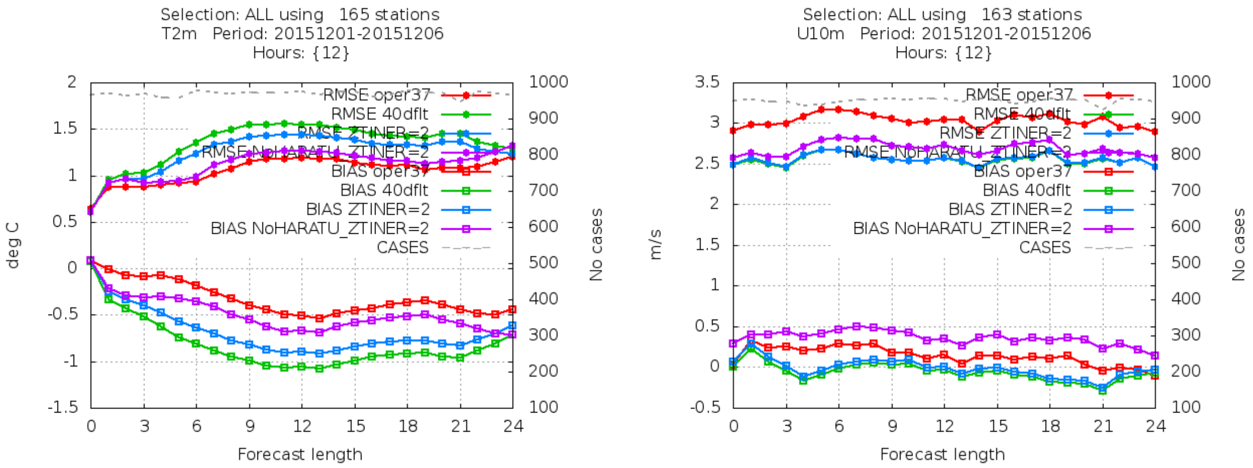

(a) (b)

Figure 9: Point verification of (a) 2 m temperature and (b) 10 m wind-speed for the wet December 2015 case for various experiments with ZTINER in the SURFEX assimilation: constant ZTINER value of 2 (ZTINER=2, blue); HARATU=no, constant ZTINER value of 2 (NoHARATU_ZTINER=2, magenta).

scheme was tested. This is controlled by a CROUGH setting, which is ‘none’ by default; we tested the CROUGH=‘Z01D’ scheme, which does not depend on wind direction.

Results from these experiments are shown in Fig. 10 for the wet and windy test period of December 2015. In these we focussed on cycle 40h1.1 only, with default set-up (40dflt) now shown in red, and looked at the influence of combinations of the changes described above, denoted as follows: ‘opD’ (operational XCDRAG value), ‘LAI’ (LAI drag) and ‘CR’ (orographic roughness). We first note the 2 m temperature verification scores in Fig. 10a. The drag changes have no detrimental effects: the benefits of the NHZ2 set-up hold.

The scores for 10 m wind-speed and maximum gusts are shown in Figs. 10b and 10c, respectively. For the 10 m wind-speed in 10b, the increased drag from the canopy and LAI lead to the best compromise of scores (NHZ2_opD_LAI, blue). Although the use of the CROUGH scheme (magenta and cyan) arguably displays a more neutral bias for the gusts in Fig. 10c, these settings are much less accurate for the average wind-speed.

The separate effects of these drag changes can be better understood by examining wind fields from individual forecasts. In Fig. 11 we take the 24-hour forecast starting from 1200 UTC on the 6$^{\text{th}}$ of December 2015 and examine the differences in 10 m wind-speed when each of the three drag options above are added to the default cycle 40h1. As expected, we see a reduction in wind-speed in all cases.

Fig. 11a shows the effect of the ‘opD’ change, i.e. increasing the canopy drag parameter XCDRAG. Looking next at 11b, the increased drag from the LAI change over grassland, we see that this affects areas not influenced by the canopy (the vegetation types from the ECOCLIMAP database are plotted in Fig. 12). Together, these changes have a reasonably uniform effect over the whole country.

In contrast, the use of the CROUGH=‘Z01D’ scheme in Fig. 11c shows a very strong weakening of the winds in mountainous areas (note the different colour scale), which greatly affects the scores at local stations. As seen already from the point verification in Fig. 10, this effect is too severe and so this change was rejected.

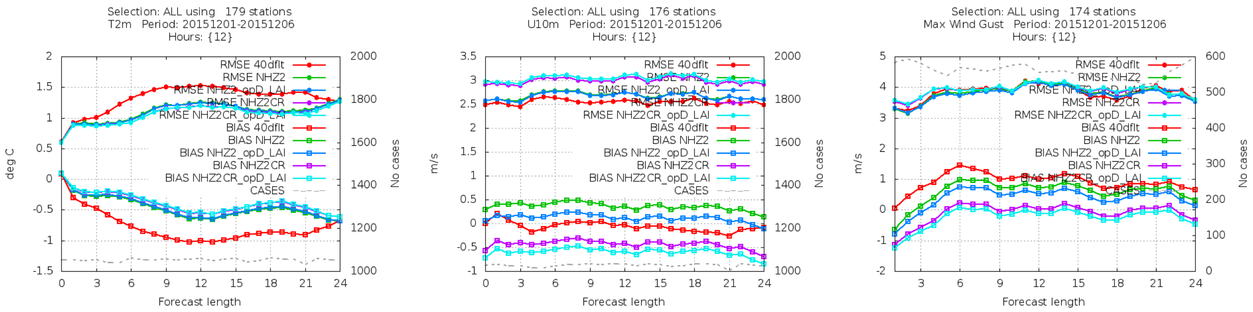

(a) (b) (c)

Figure 10: Point verification for the wet and windy December 2015 test period, for parameters (a) 2 m temperature, (b) 10 m wind-speed and (c) 10 m maximum gust. Shown are the default cycle 40h1.1 (40dflt, red) and the NHZ2 set-up (green), along with the following drag combinations included with NHZ2: XCDRAG=0.05 and increased LAI drag (NHZ2_opD_LAI, blue; 'Z01D' orographic roughness scheme (NHZ2CR, magenta); all three drag options (NHZ2CR_opD_LAI, cyan)

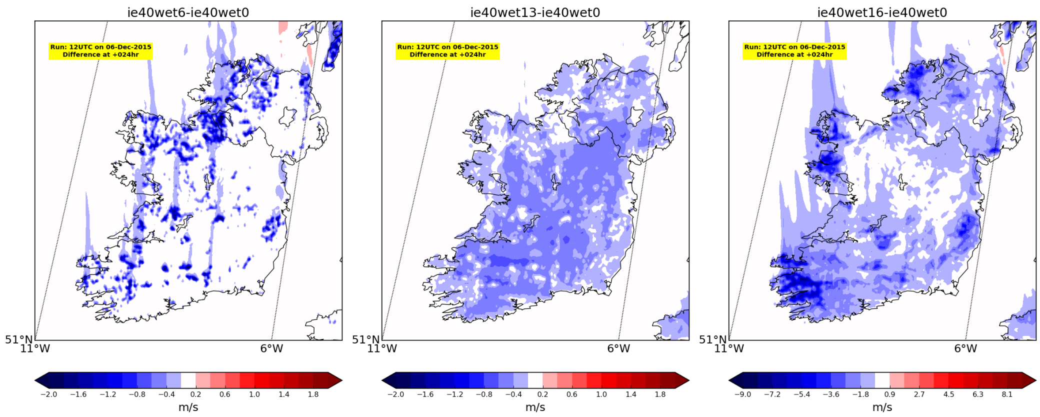

(a) (b) (c)

Figure 11: Differences in 10 m wind-speed, for 2015120612+024 forecasts, when each drag change is added to the default cycle 40h1: (a) opD minus default; (b) LAI minus default; (c) CR minus default. Note the differing scale in (c).

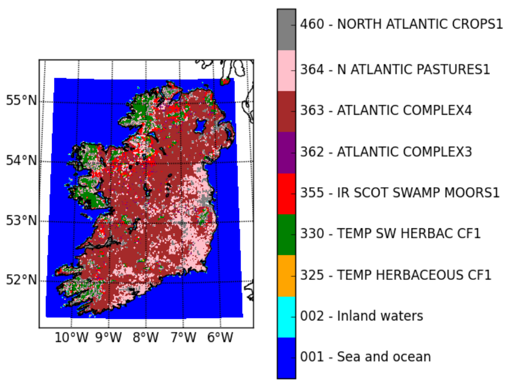

Figure 12: Vegetation types in ECOCLIMAP Version 2.2

5 Data assimilation

Data assimilation techniques are used to provide the forecast model with an initial state of the surface and atmosphere. Observations and *a priori* model-state information are combined to produce the most likely initial state. A full description of data assimilation specific to HARMONIE-AROME is provided in Whelan et al. (2018).

In HARMONIE-AROME optimal interpolation (OI) is used to update the surface and soil parameters. The OI implementation is described in Giard and Bazile (2000) and implemented in the SURFEX model (Masson et al., 2013). Only observations at the analysis time are assimilated by the surface OI assimilation scheme. Screen level observations of temperature and humidity are assimilated by the HARMONIE-AROME OI (Fig. 13a) with the increments produced by these observations used to produced an analysis of soil temperature and moisture.

Three-dimensional variational (3D-Var) data assimilation is used to produce the upper-air analysis for each forecast cycle and is described in Fischer et al. (2005) and Courtier et al. (1998). An analysis window of three hours centred on the analysis time is used by 3D-Var with observations reported within this time-window assimilated. The derivation of the background error statistics used by HARMONIE-AROME 3D-Var is described in Brousseau et al. (2011). The error statistics were calculated using differences between 6-hour forecasts from a four-member ensemble of downscaled IFS ensemble forecasts run for 40 cycles. Conventional observations from SYNOP, SHIP, BUOY, AIREP, TEMP and PILOT reports are assimilated, Fig. 13b.

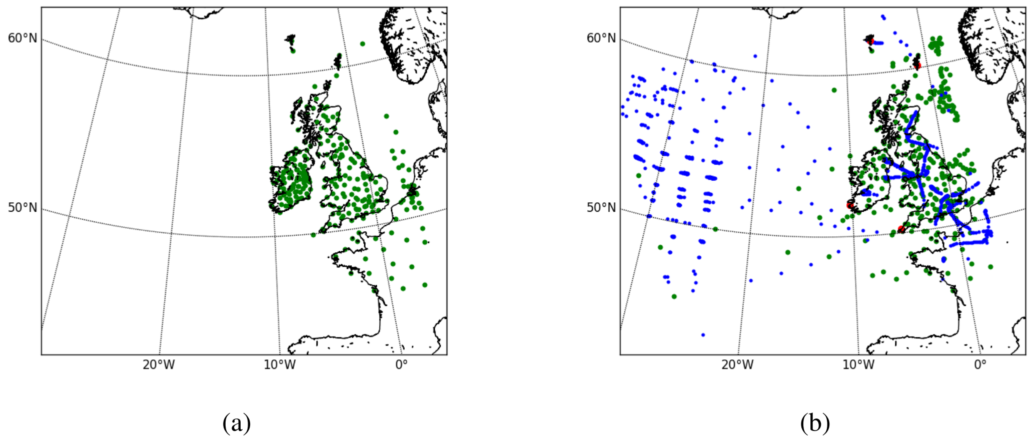

Figure 13: Observations assimilated by HARMONIE-AROME (a) OI and (b) 3D-Var data assimilation for a typical 1200 UTC cycle. SYNOP (surface land and sea) observations are shown in blue, AIREP (aircraft) in blue and TEMP (radiosondes) in red.

6 Final model assessment

Following the analysis and experiences described in Section 4, the changes described in Table 2 were made to the default cycle 40h1.1 to create an ‘optimal’ pre-operational configuration, hereafter referred to as ie40.

Change	Affected file	Description
HARATU=no	sms/config_exp.h	Turbulence scheme, i.e. use default instead of HARATU
ZTINER=2.0	src/surfex/ASSIM/oi_cacsts.F90	Temperature increment in surface analysis
ZH $\leftarrow$ ZLAI/4 for grassland	src/surfex/SURFEX/z0v_from_lai.F90	Increased drag from grassland (default is ZLAI/6)
XCDRAG=0.05	nam/surfex_namelists.pm	Canopy drag coefficient (value used in oper37)

Table 2: Changes made to default cycle 40h1.1 for pre-operational testing.

Month-long tests were carried out on the proposed larger domain (Fig.1) using 3D-Var data assimilation. The year 2014 was chosen as a test period, having a stormy winter (particularly February) and a warm summer. Five month-long experiments were run: February, April, June, September and November. Three-hour cycling was used, with 24-hour forecasts at 0000 UTC and 1200 UTC. Point verification for eight parameters are shown for the 0000 UTC forecasts in Fig. 14 and for the 1200 UTC forecasts in Fig. 15. All five months are combined here, comparing the operational cycle 37h1.1 (oper37, in red) with the proposed cycle 40h1.1 set-up (ie40, in green) The individual months are shown separately in Appendix A.

Considering both Figs. 14 and 15, we see that, in general, ie40 has a neutral or slightly positive impact on the verification scores. The 10 m wind-speed scores (Figs. 14a and 15a) show an improvement in ie40. While the ie40 cold bias is visible in 2 m temperature (Figs. 14c and 15c), the RMSE values are comparable with oper37. Additionally, there is an improvement in the bias of 2 m dewpoint temperature (Figs. 14d and 15d), likely due to the improved accuracy in humidity (Figs. 14e and 14f, 15e and 15f).

While point verification is useful for measuring average performance over a period of time, it is also instructive to examine particular forecast examples. A selection of cases were used to assess model performance in situations involving high winds, low temperatures, poor visibility and rainfall. Full details are given in Appendix B. In general these show neutral to slighty better results from ie40, with no particular deficiencies or problems being apparent.

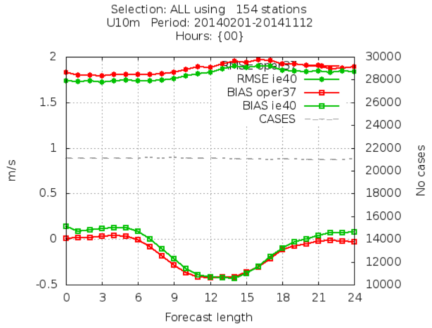

(a)

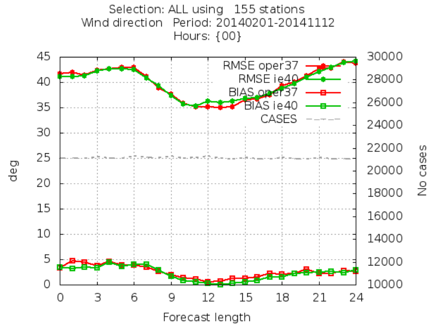

(b)

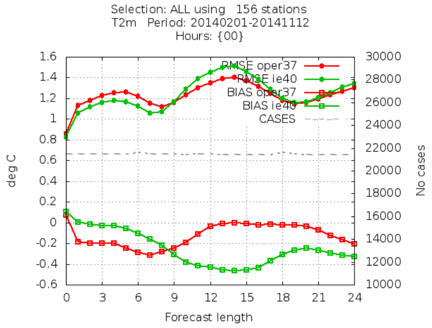

(c)

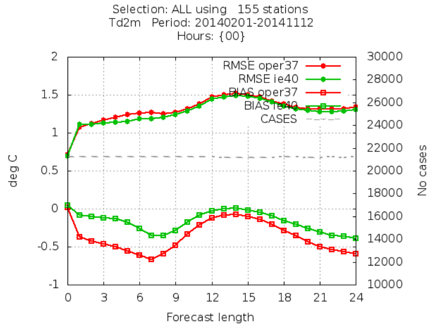

(d)

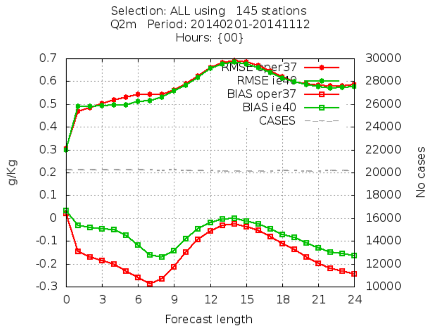

(e)

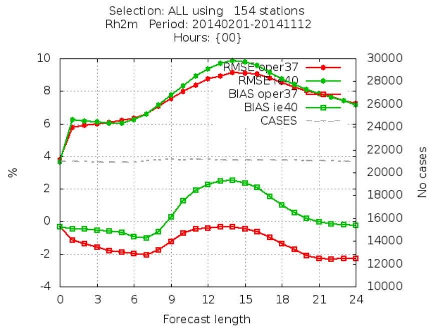

(f)

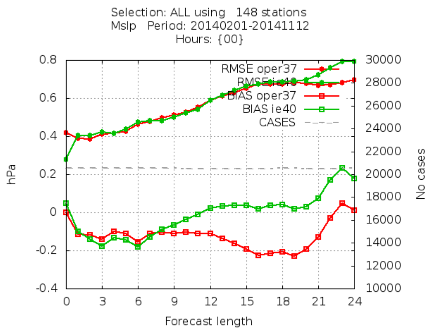

(g)

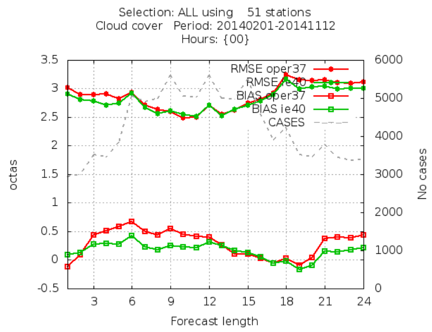

(h)

Figure 14: Point verification of 0000 UTC forecasts for all month-long tests combined. Parameters are: (a) 10 m wind-speed, (b) 10 m wind direction, (c) 2 m temperature, (d) 2 m dewpoint temperature, (e) 2 m specific humidity, (f) 2 m relative humidity, (g) mean sea-level pressure, and (h) cloud cover.

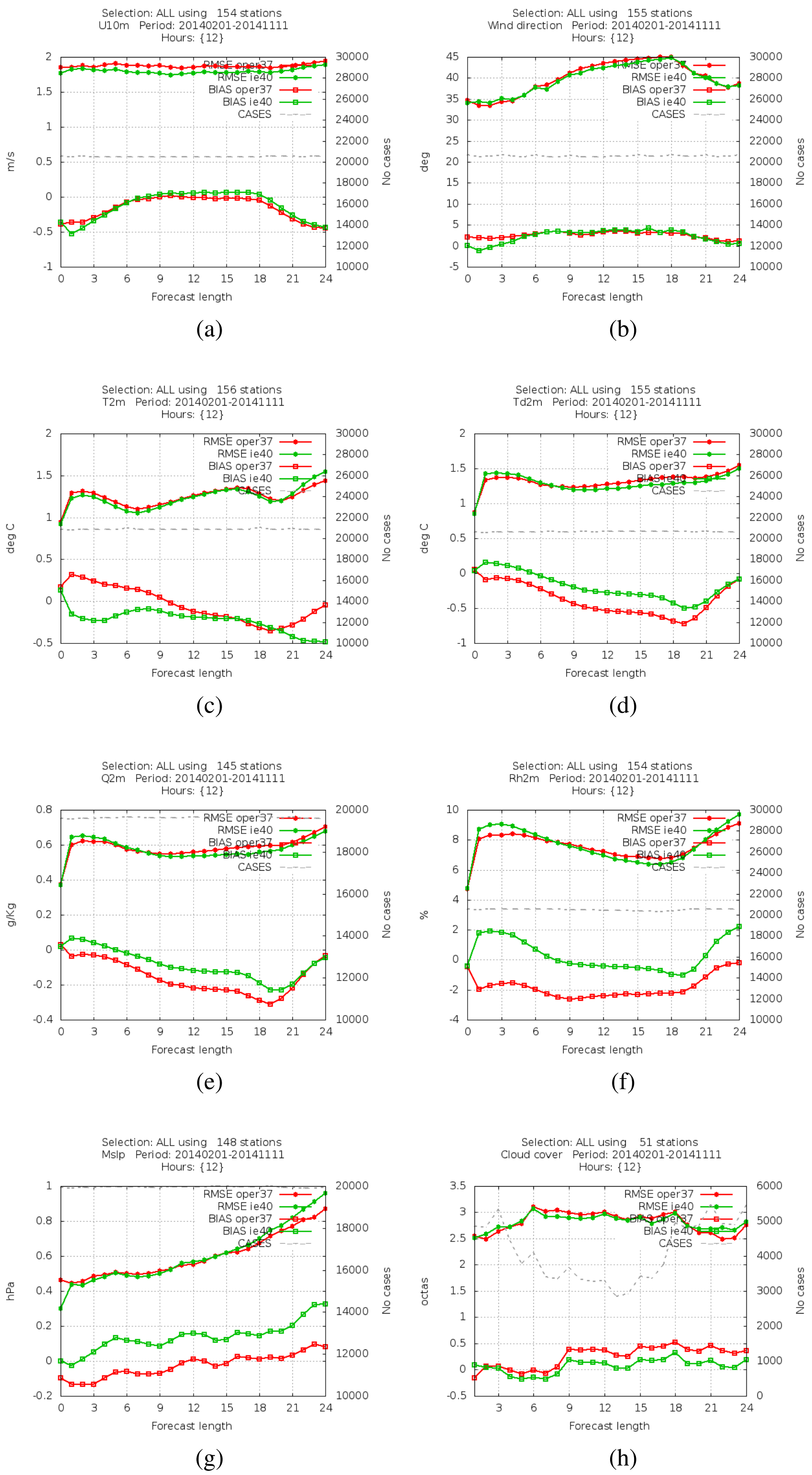

Figure 15: Point verification of 1200 UTC forecasts for all month-long tests combined. Parameters are: (a) 10 m wind-speed, (b) 10 m wind direction, (c) 2 m temperature, (d) 2 m dewpoint temperature, (e) 2 m specific humidity, (f) 2 m relative humidity, (g) mean sea-level pressure, and (h) cloud cover.

7 Operational implementation

The tested new set-up (ie40) with the changes listed in Table 2 was given the experiment name HAR40 and put into parallel operational cycling for a number of months to spin-up the surface processes. The switch-over to operational use was carried out for the 1200 UTC forecast on the 1st of May 2018.

Examples of forecasts from the new HAR40, compared with the old 37h1.1, are shown in Fig.16. The benefit of the larger domain is quite apparent, providing information on a much larger spatial scale. In Fig. 17 verification results are presented for the whole of May 2018, the first month of full operations for HAR40. Overall the scores are broadly neutral, showing both slight improvements (e.g. in MSLP and relative humidity biases, Figs. 17g and 17f) and some slightly negative effects (e.g. dew-point bias, Fig. 17d).

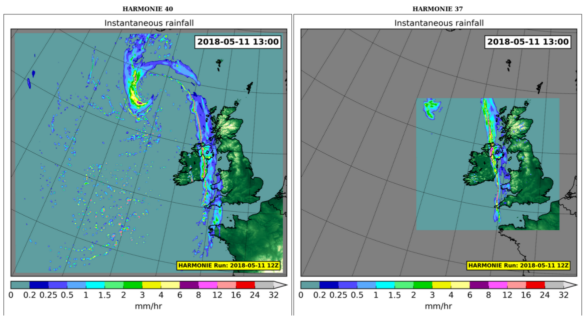

(a)

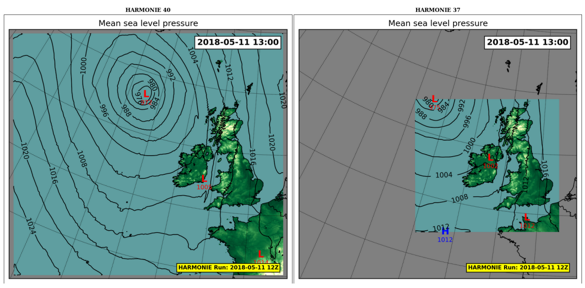

(b)

Figure 16: New 40h1.1 running operationally and compared with the old 37h1.1, showing sample forecasts of (a) precipitation, and (b) MSLP.

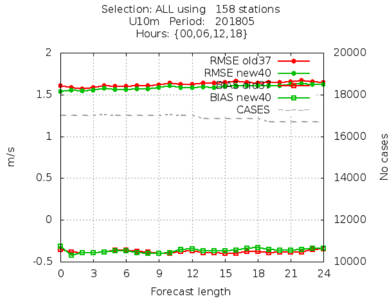

(a)

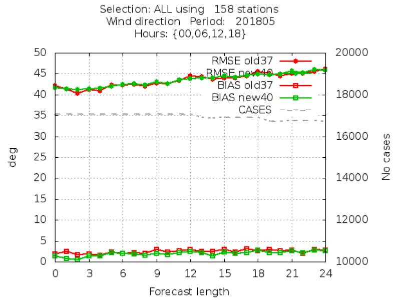

(b)

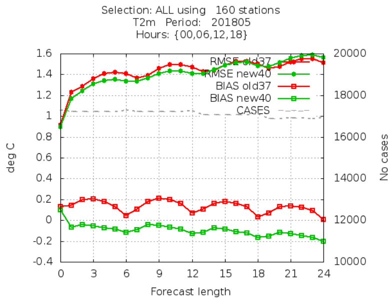

(c)

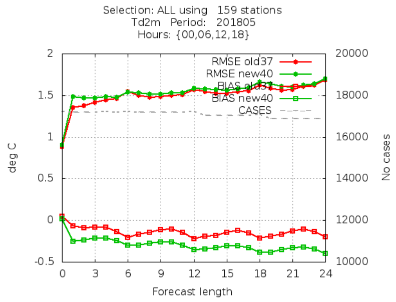

(d)

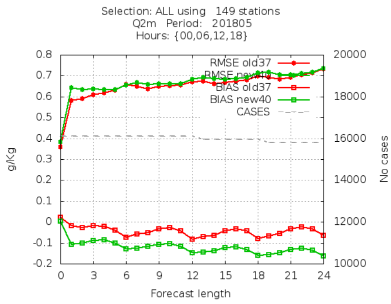

(e)

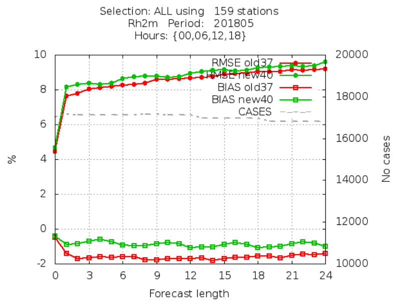

(f)

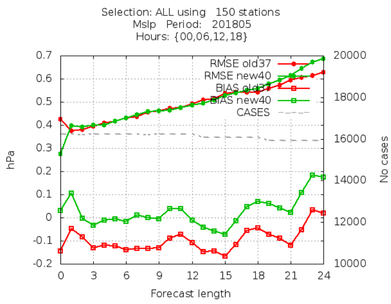

(g)

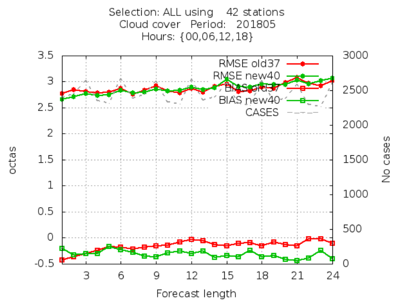

(h)

Figure 17: Point verification of forecasts for May 2018, comparing the old operational cycle 37h1.1 (old37, red) with the new the (new40, green) in its first operational month. Parameters are: (a) 10 m wind-speed, (b) 10 m wind direction, (c) 2 m temperature, (d) 2 m dewpoint temperature, (e) 2 m specific humidity, (f) 2 m relative humidity, (g) mean sea-level pressure, and (h) cloud cover.

8 Outlook

There are many further enhancements possible with the cycle 40h1.1 system that may improve the short-range forecasts produced by HARMONIE-AROME. With regard to model dynamics there is an option to increase computational efficiency by moving to a quadratic spectral grid (Bengtsson et al., 2017). This is not currently in operational use, but the option remains a possibility for future upgrades. Currently the Irish implementation of cycle 40h1.1 only assimilates conventional observations. With cy40h1.1 it is possible to assimilate satellite radiances, satellite derived winds, aircraft derived observations, radar reflectivities and observations derived from GPS data. In the near future it is planned to assimilate ASCAT ocean surface winds and satellite radiances.

The next major operational NWP change planned will be the introduction of a convection-permitting ensemble system, to be known as the Irish Regional Ensemble Prediction System (IREPS). IREPS will use the deterministic HAR40 forecast as its control with the 10 extra members being generated using the Scaled Lagged Average Forecasting (SLAF) method already in use within the HarmonEPS community (Frogner et al., 2018, manuscript in preparation). IREPS will also make use of surface perturbations following the work of Bouttier et al. (2015).

References

Bengtsson, L., Andrae, U., Aspelien, T., Batrak, Y., Calvo, J., de Rooy, W., Gleeson, E., Hansen-Sass, B., Homleid, M., Hortal, M., Ivarsson, K.-I., Lenderink, G., Niemelä, S., Nielsen, K. P., Onvlee, J., Rontu, L., Samuelsson, P., Muñoz, D. S., Subias, A., Tijm, S., Toll, V., Yang, X., and Køltzow, M. Ø. (2017). The HARMONIE-AROME Model Configuration in the ALADIN-HIRLAM NWP System. *Mon. Wea. Rev.*, 145(5):1919–1935.

Bouttier, F., Vié, B., Nuissier, O., and Ménétrier, B. (2015). Sensitivity of the AROME ensemble to initial and surface perturbations during HyMeX. *Q.J.R. Meteorol. Soc.*, 142:390–403.

Brousseau, P., Berre, L., Bouttier, F., and Desroziers, G. (2011). Background-error covariances for a convective-scale data-assimilation system: AROME-France 3D-Var. *Q.J.R. Meteorol. Soc.*, 137(655):409–422.

Courtier, P., Andersson, E., Heckley, W., Vasiljevic, D., Hamrud, M., Hollingsworth, A., Rabier, F., Fisher, M., and Pailleux, J. (1998). The ECMWF implementation of three-dimensional variational assimilation (3D-Var). I: Formulation. *Q.J.R. Meteorol. Soc.*, 124(550):1783–1807.

Fischer, C., Montmerle, T., Berre, L., Auger, L., and Ştefănescu, S. E. (2005). An overview of the variational assimilation in the ALADIN/France numerical weather-prediction system. *Q.J.R. Meteorol. Soc.*, 131(613):3477–3492.

Giard, D. and Bazile, E. (2000). Implementation of a New Assimilation Scheme for Soil and Surface Variables in a Global NWP Model. *Mon. Wea. Rev.*, 128(4):997–1015.

HIRLAM (2016). Harmonie 40h1.1 Release Notes. `https://hirlam.org/trac/wiki/ReleaseNotes/harmonie-40h1.1`. Accessed October 4, 2018.

Masson, V., Le Moigne, P., Martin, E., Faroux, S., Alias, A., Alkama, R., Belamari, S., Barbu, A., Boone, A., Bouyssel, F., Brousseau, P., Brun, E., Calvet, J.-C., Carrer, D., Decharme, B., Delire, C., Donier, S., Essaouini, K., Gibelin, A.-L., Giordani, H., Habets, F., Jidane, M., Kerdraon, G., Kourzeneva, E., Lafaysse, M., Lafont, S., Lebeaupin Brossier, C., Lemonsu, A., Mahfouf, J.-F., Marguinaud, P., Mokhtari, M., Morin, S., Pigeon, G., Salgado, R., Seity, Y., Taillefer, F., Tanguy, G., Tulet, P., Vincendon, B., Vionnet, V., and Voldoire, A. (2013). The SURFEXv7.2 land and ocean surface platform for coupled or offline simulation of earth surface variables and fluxes. *Geosci. Model Dev.*, 6(4):929–960.

McGrath, R. (2015). Impact of Storm Darwin on Ireland: description of the event and assessment of weather forecasts. Technical Report 64, Met Éireann.

Termonia, P., Fischer, C., Bazile, E., Bouyssel, F., Brožková, R., Bénard, P., Bochenek, B., Degrauwe, D., Derkova, M., El Khatib, R., Hamdi, R., Mašek, J., Pottier, P., Pristov, N., Seity, Y., Smolíková, P., Spaniel, O., Tudor, M., Wang, Y., Wittmann, C., and Joly, A. (2018). The ALADIN System and its Canonical Model Configurations AROME CY41T1 and ALARO CY40T1. *Geosci. Model Dev.*, 11:257–281.

Whelan, E., Gleeson, E., and Hanley, J. (2018). An Evaluation of MÉRA, a High-Resolution Mesoscale Regional Reanalysis. *J. Appl. Meteor. Climatol.*, 57(9):2179–2196.

A Month-long verification scores

In Section 6, month-long experiments with the pre-operational cycle 40h1.1 were described. Five months were chosen in 2014 for comparison with the operational 37h1.1. We show here in Figs. 18 to 27 the verification scores for the 0000 UTC and 1200 UTC forecasts for each of the five months separately.

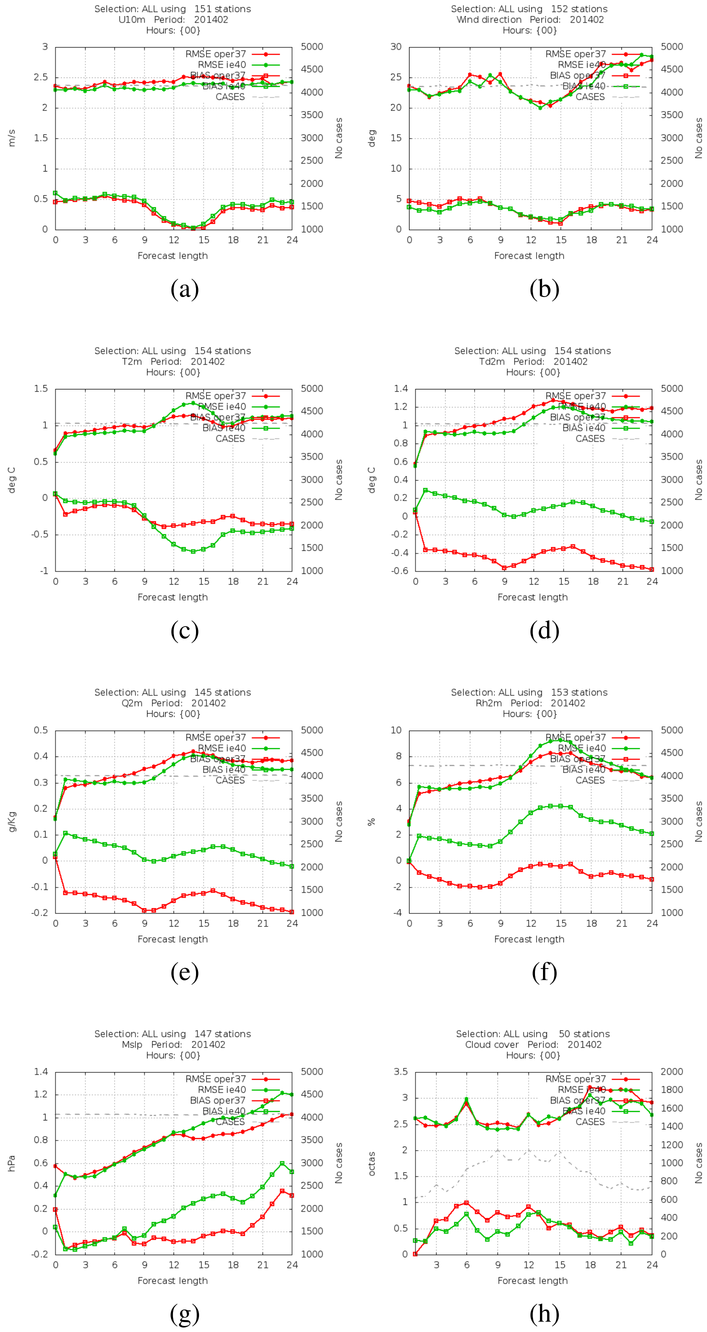

Figure 18: Point verification of 0000 UTC forecasts for February 2014. Parameters are: (a) 10 m wind-speed, (b) 10 m wind direction, (c) 2 m temperature, (d) 2 m dewpoint temperature, (e) 2 m specific humidity, (f) 2 m relative humidity, (g) mean sea-level pressure, and (h) cloud cover.

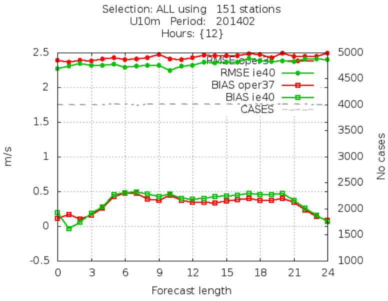

(a)

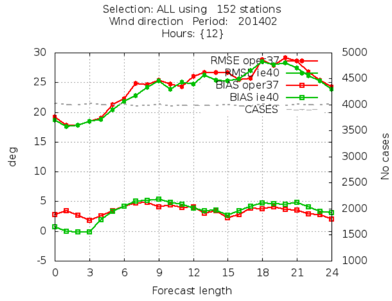

(b)

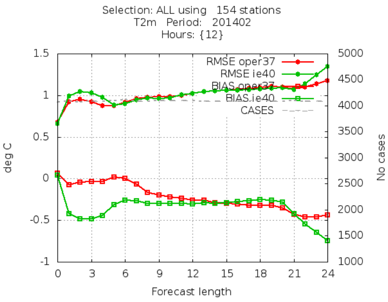

(c)

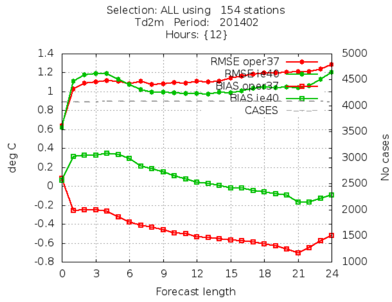

(d)

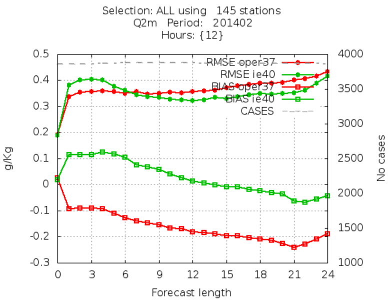

(e)

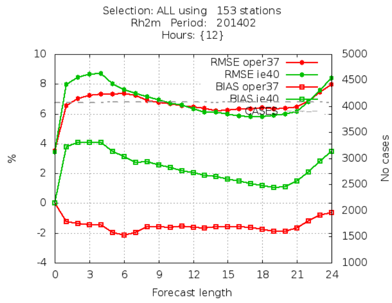

(f)

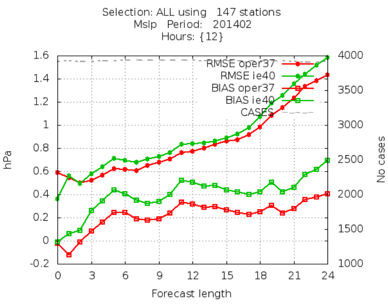

(g)

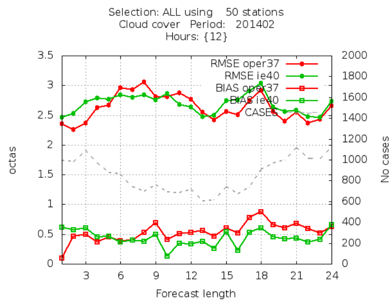

(h)

Figure 19: Point verification of 1200 UTC forecasts for February 2014. Parameters are: (a) 10 m wind-speed, (b) 10 m wind direction, (c) 2 m temperature, (d) 2 m dewpoint temperature, (e) 2 m specific humidity, (f) 2 m relative humidity, (g) mean sea-level pressure, and (h) cloud cover.

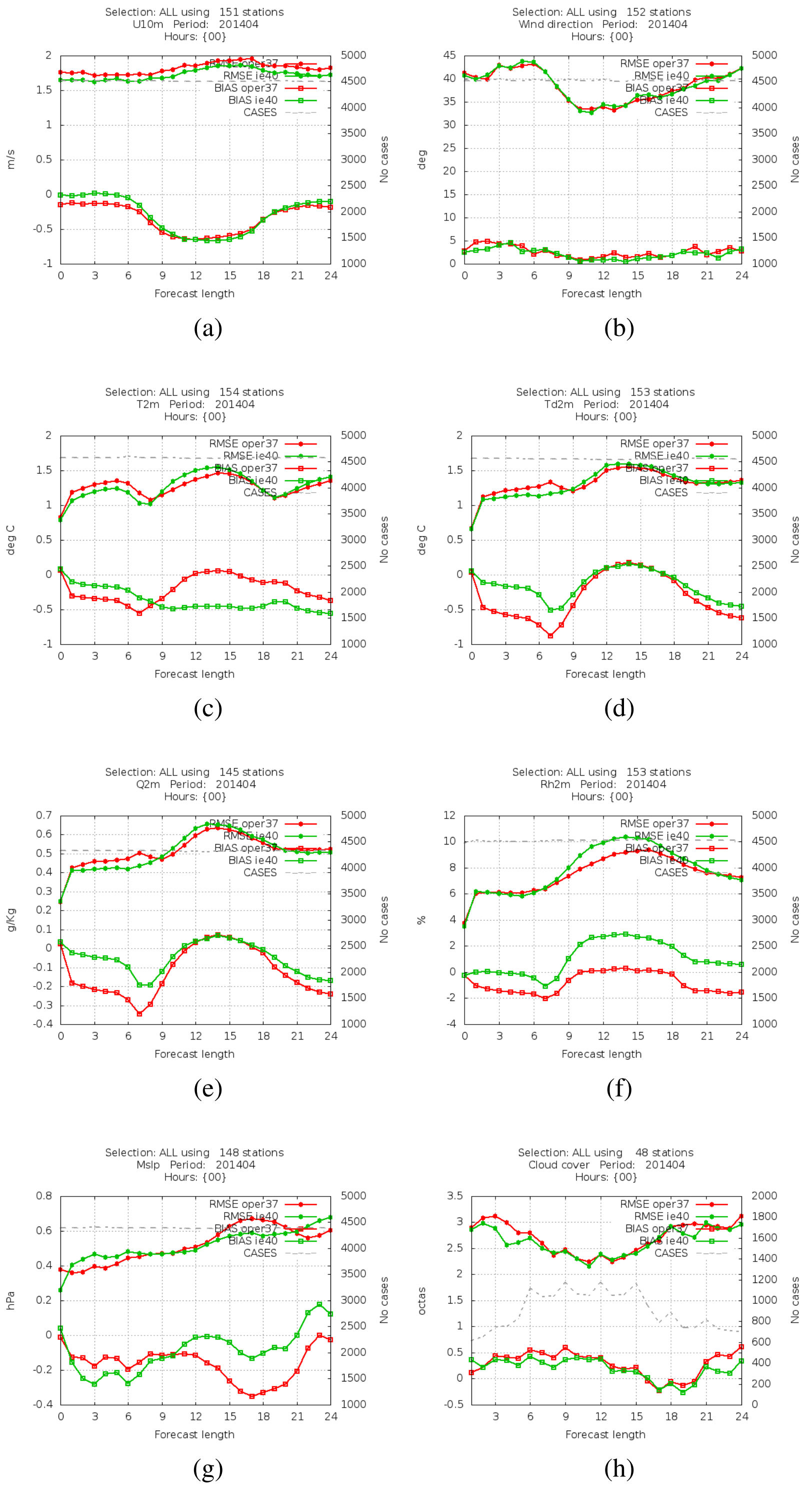

Figure 20: Point verification of 0000 UTC forecasts for April 2014. Parameters are: (a) 10 m wind-speed, (b) 10 m wind direction, (c) 2 m temperature, (d) 2 m dewpoint temperature, (e) 2 m specific humidity, (f) 2 m relative humidity, (g) mean sea-level pressure, and (h) cloud cover.

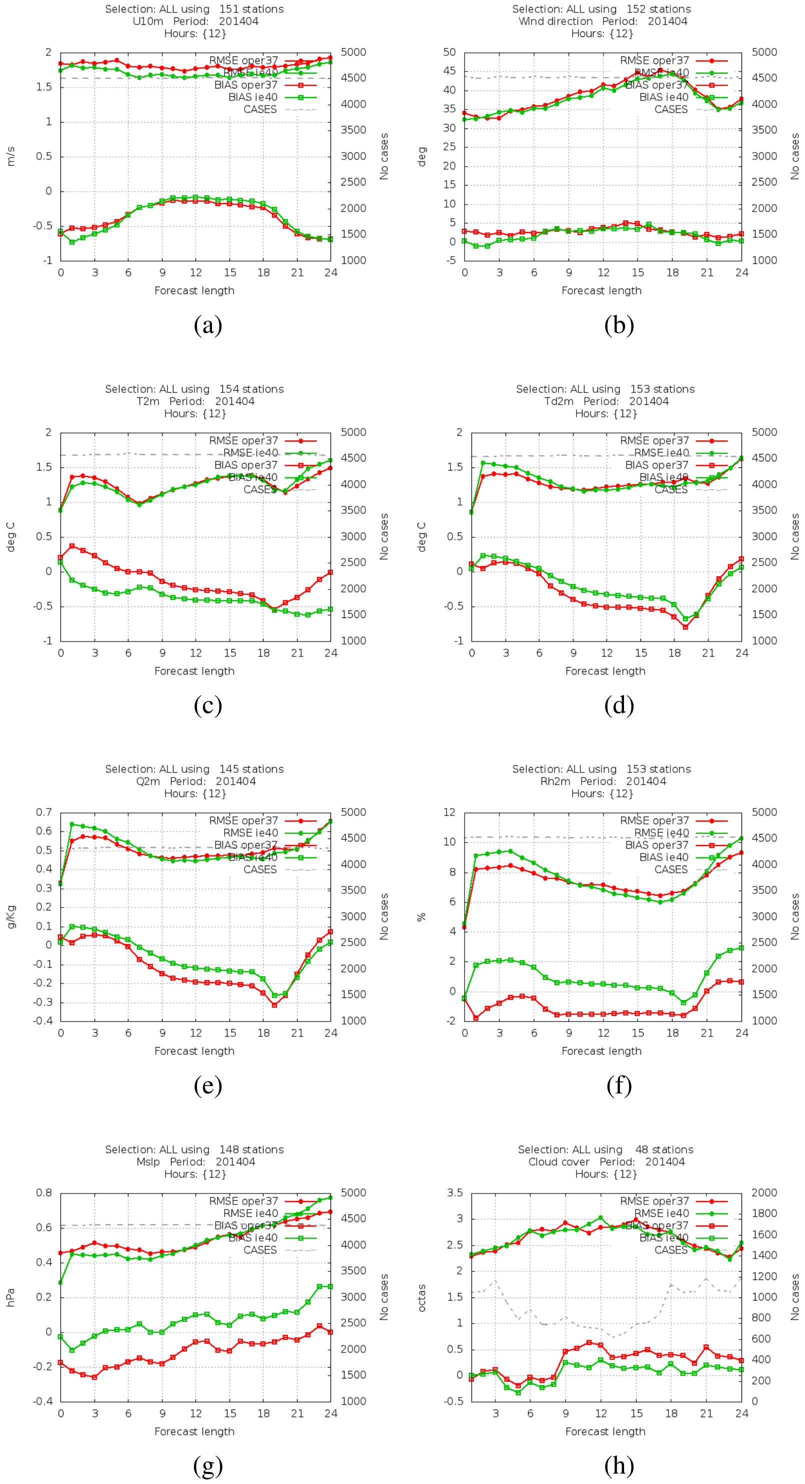

Figure 21: Point verification of 1200 UTC forecasts for April 2014. Parameters are: (a) 10 m wind-speed, (b) 10 m wind direction, (c) 2 m temperature, (d) 2 m dewpoint temperature, (e) 2 m specific humidity, (f) 2 m relative humidity, (g) mean sea-level pressure, and (h) cloud cover.

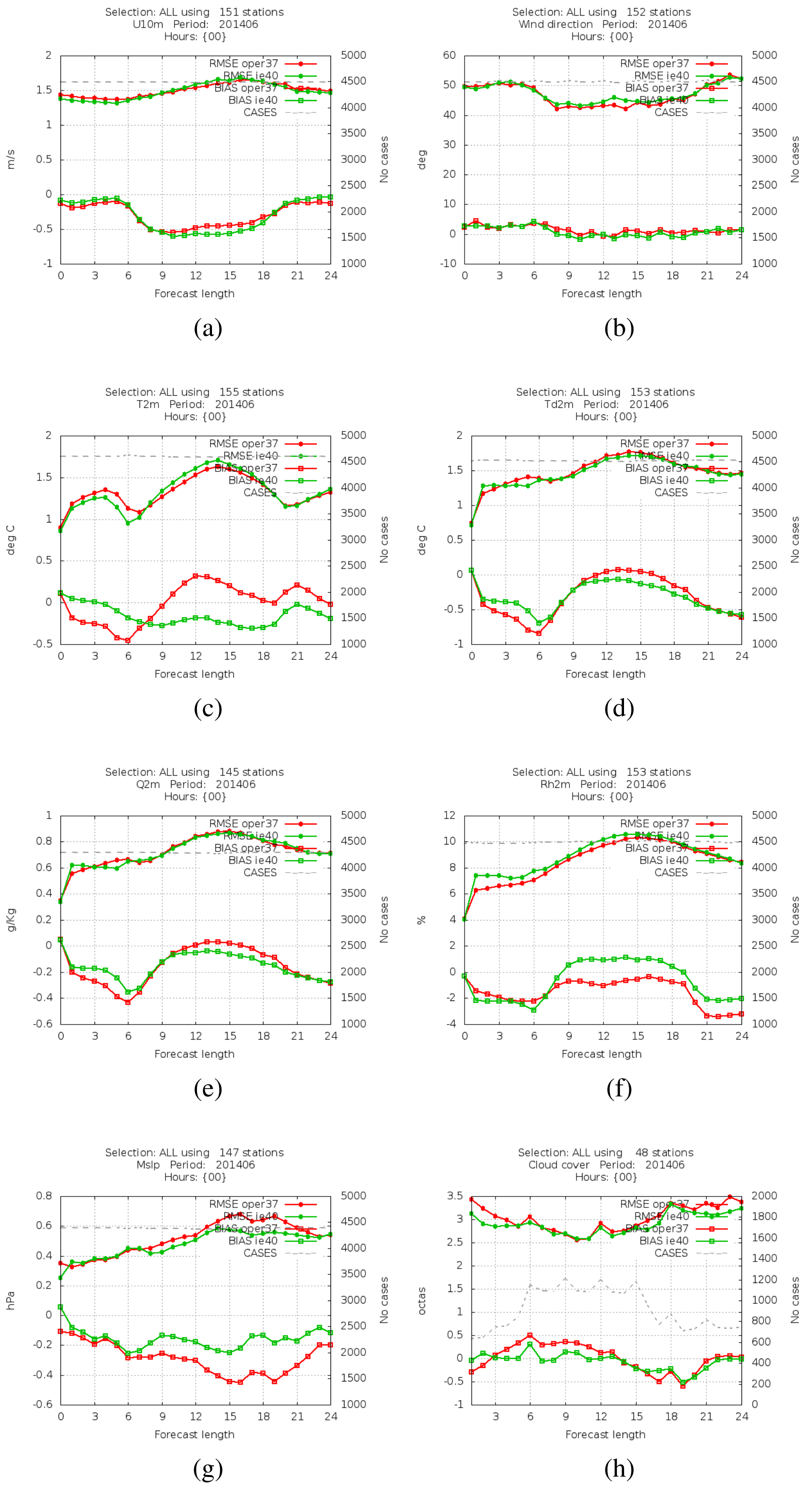

Figure 22: Point verification of 0000 UTC forecasts for June 2014. Parameters are: (a) 10 m wind-speed, (b) 10 m wind direction, (c) 2 m temperature, (d) 2 m dewpoint temperature, (e) 2 m specific humidity, (f) 2 m relative humidity, (g) mean sea-level pressure, and (h) cloud cover.

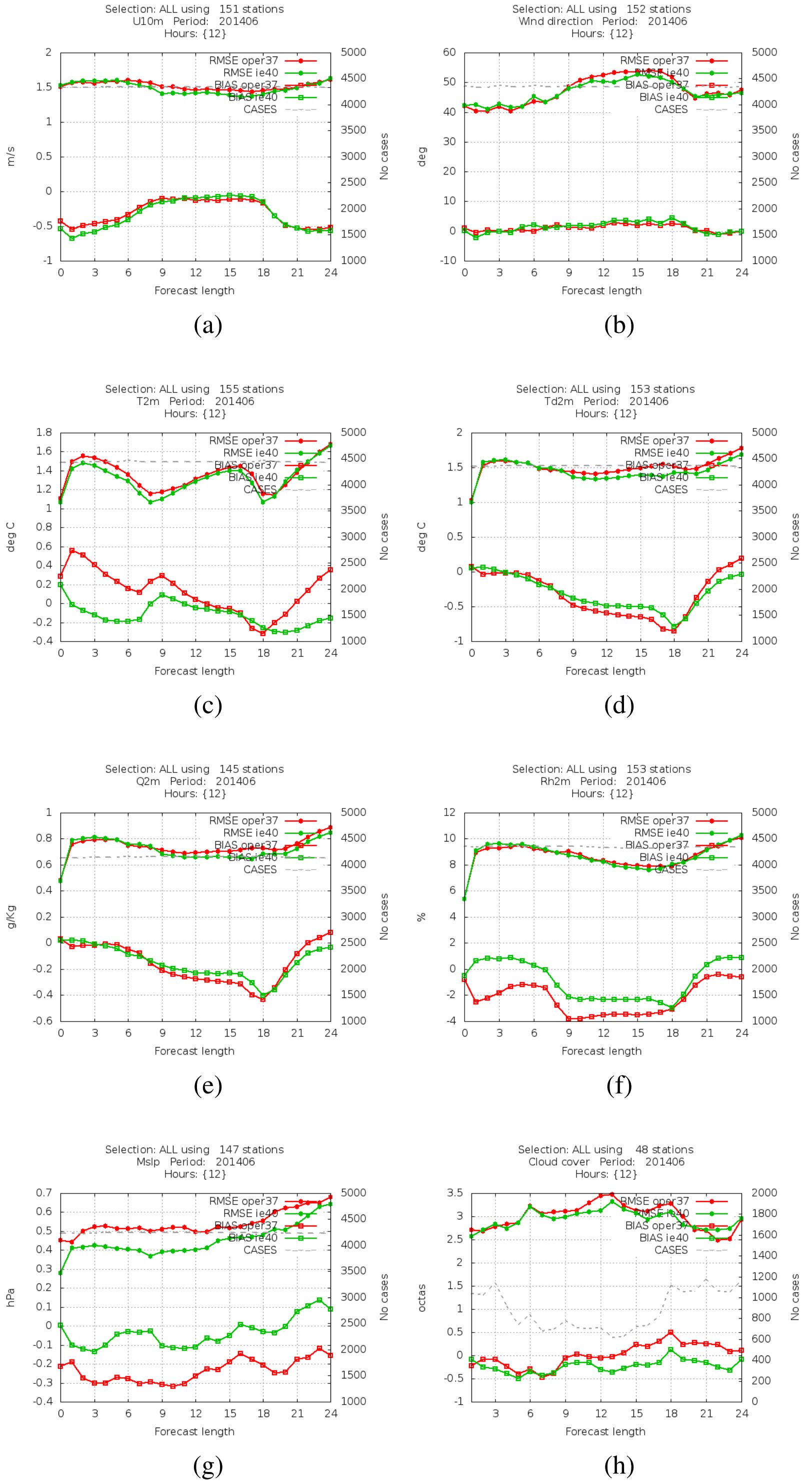

Figure 23: Point verification of 1200 UTC forecasts for June 2014. Parameters are: (a) 10 m wind-speed, (b) 10 m wind direction, (c) 2 m temperature, (d) 2 m dewpoint temperature, (e) 2 m specific humidity, (f) 2 m relative humidity, (g) mean sea-level pressure, and (h) cloud cover.

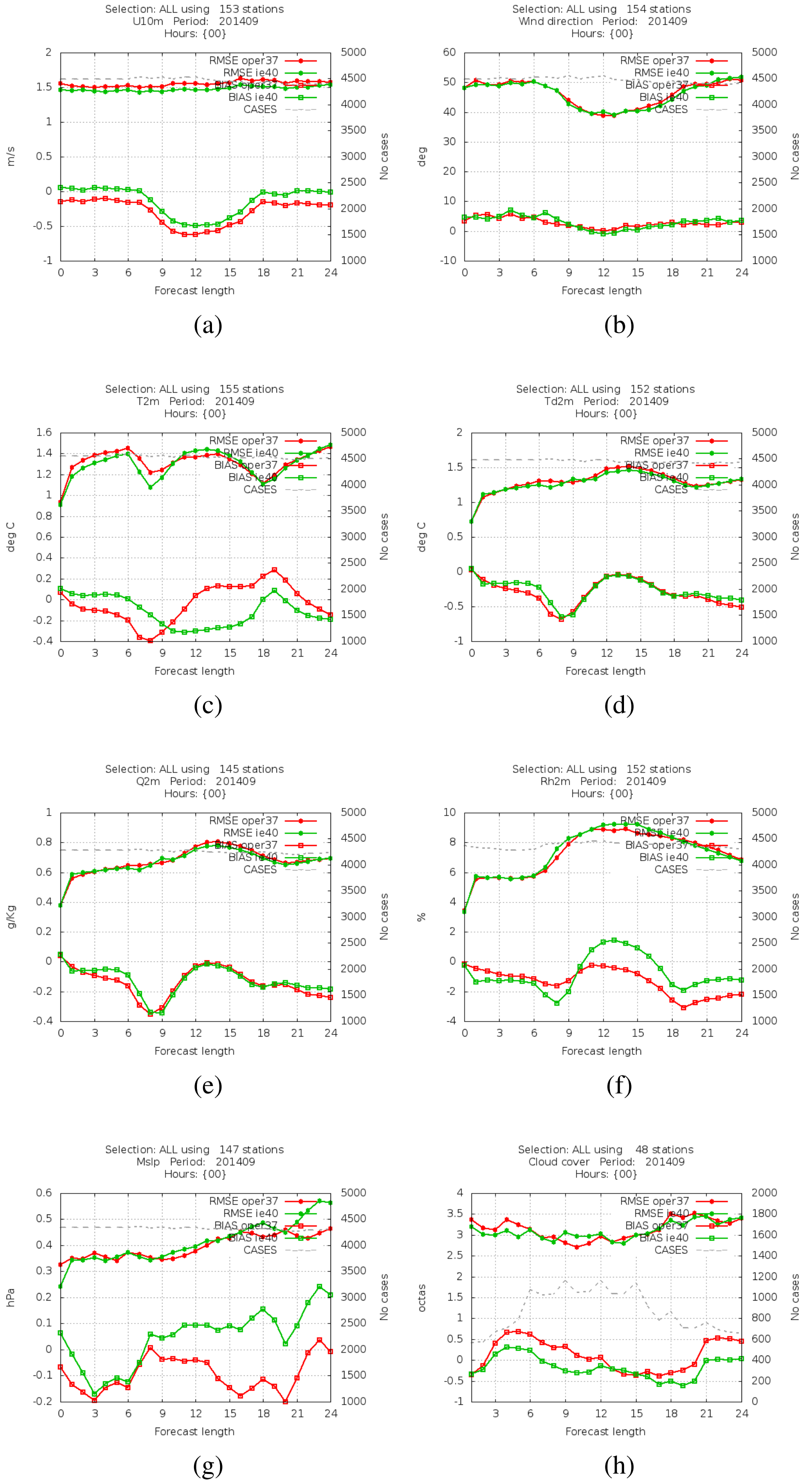

Figure 24: Point verification of 0000 UTC forecasts for September 2014. Parameters are: (a) 10 m wind-speed, (b) 10 m wind direction, (c) 2 m temperature, (d) 2 m dewpoint temperature, (e) 2 m specific humidity, (f) 2 m relative humidity, (g) mean sea-level pressure, and (h) cloud cover.

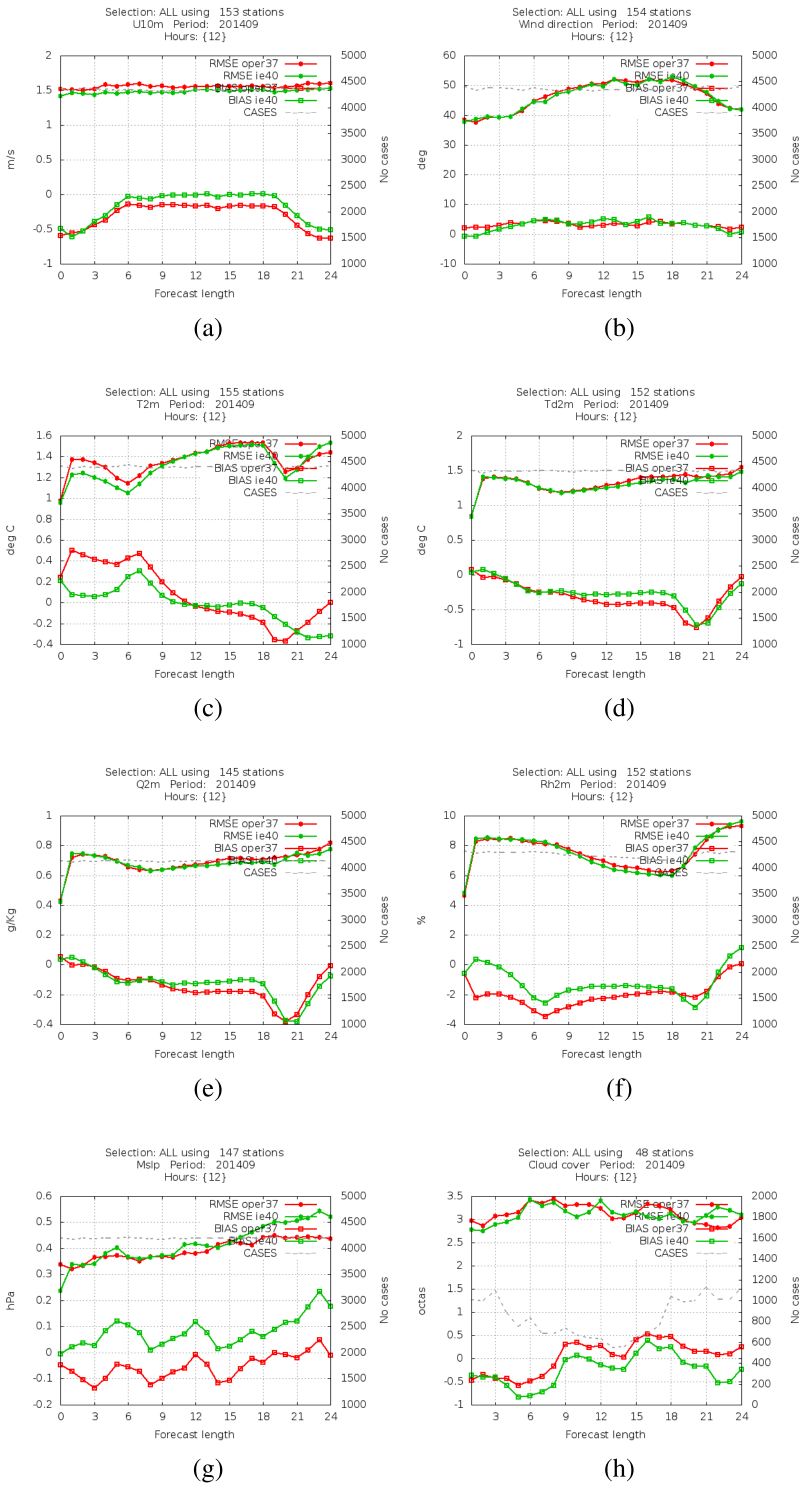

Figure 25: Point verification of 1200 UTC forecasts for September 2014. Parameters are: (a) 10 m wind-speed, (b) 10 m wind direction, (c) 2 m temperature, (d) 2 m dewpoint temperature, (e) 2 m specific humidity, (f) 2 m relative humidity, (g) mean sea-level pressure, and (h) cloud cover.

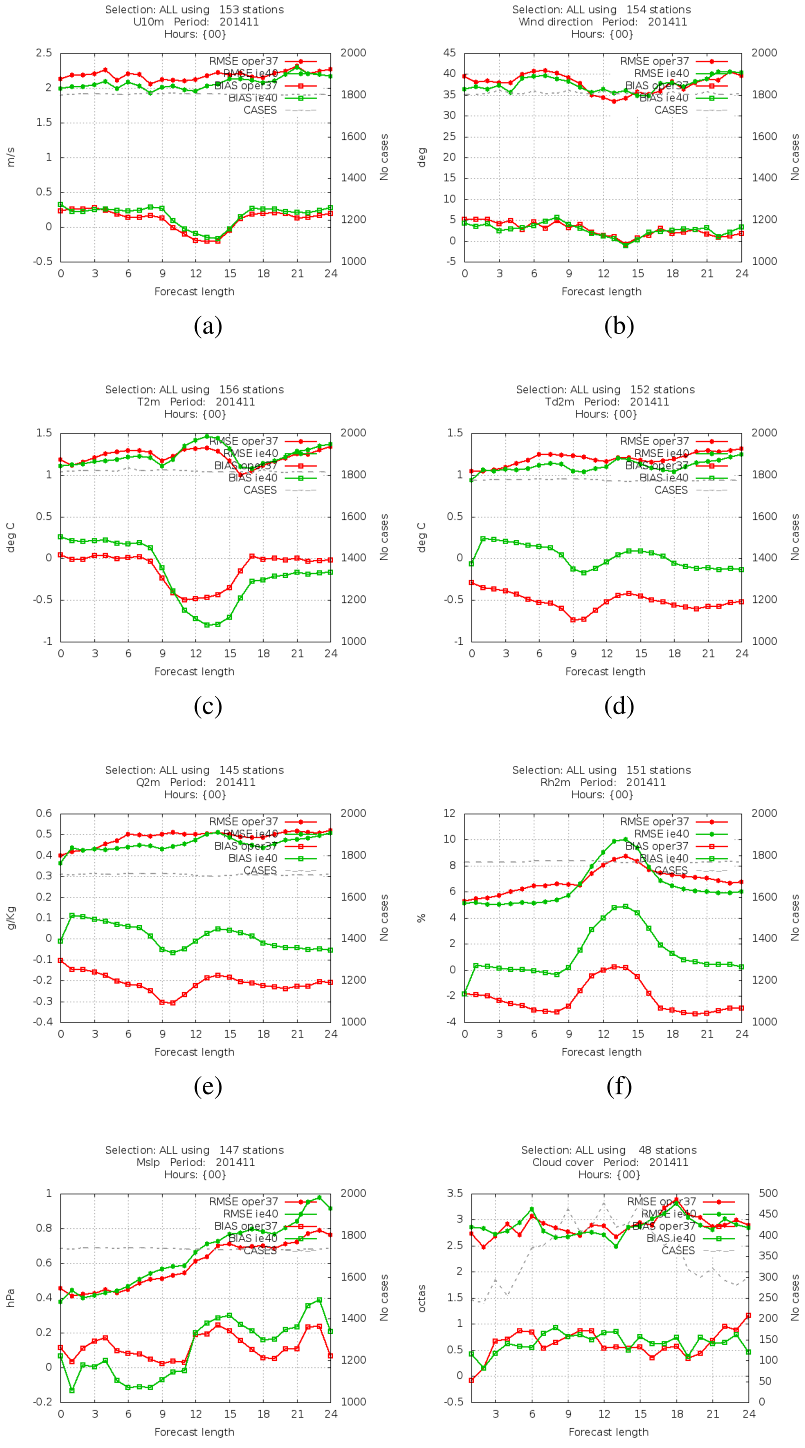

(a) (b)

(c) (d)

(e) (f)

(g) (h)

Figure 26: Point verification of 0000 UTC forecasts for November 2014. Parameters are: (a) 10 m wind-speed, (b) 10 m wind direction, (c) 2 m temperature, (d) 2 m dewpoint temperature, (e) 2 m specific humidity, (f) 2 m relative humidity, (g) mean sea-level pressure, and (h) cloud cover.

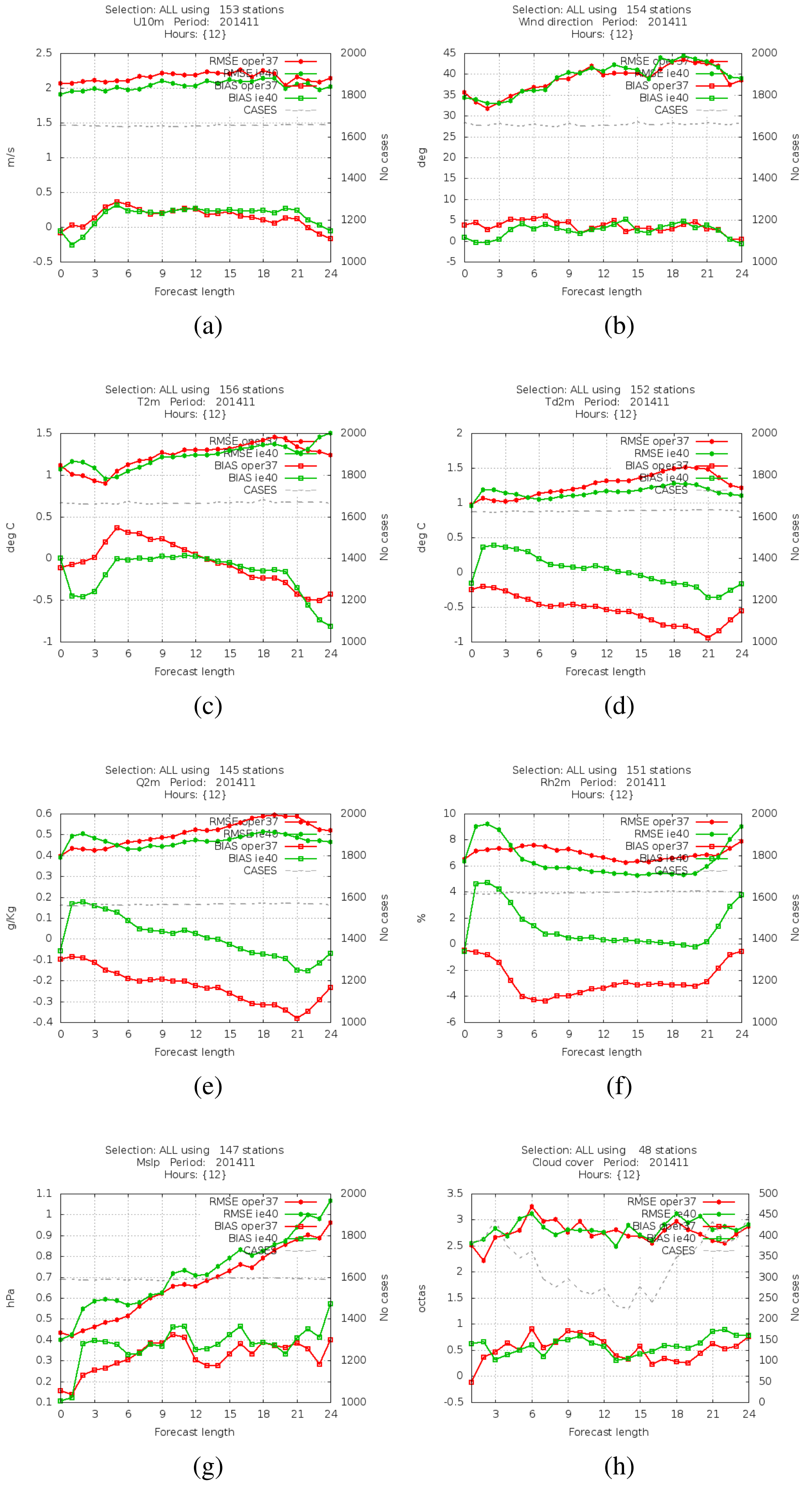

Figure 27: Point verification of 1200 UTC forecasts for November 2014. Parameters are: (a) 10 m wind-speed, (b) 10 m wind direction, (c) 2 m temperature, (d) 2 m dewpoint temperature, (e) 2 m specific humidity, (f) 2 m relative humidity, (g) mean sea-level pressure, and (h) cloud cover.

B Case studies

B.1 Storm Darwin: 12$^{\text{th}}$ of February 2014

Storm Darwin hit Ireland on the 12$^{\text{th}}$ of February, 2014. The storm, its impacts and the operational model guidance available at the time were previously analysed in McGrath (2015).

In Fig. 28 we compare the performance of the old oper37 with the new ie40 at selected stations in the south-west, where some of the most severe winds were experienced. The observed and hourly 10 m wind-speeds on the 12th are plotted; for the forecasts, we use the 0000 UTC run from the 12$^{\text{th}}$. In general, ie40 can be seen to give a neutral to slightly better performance in this case. Looking at Valentia and Sherkin Island, Figs. 28a and 28c respectively, we see the oper37 over-predicted the strongest winds at 1200 UTC. The new ie40 shows an improvement at Valentia (Fig.28a). At Sherkin Island (Fig.28c), the two models show very similar over-predictions at 1200 UTC. However, oper37 gives the peak winds at 1100 UTC whereas ie40, while still over-predicting, is closer to the observed.

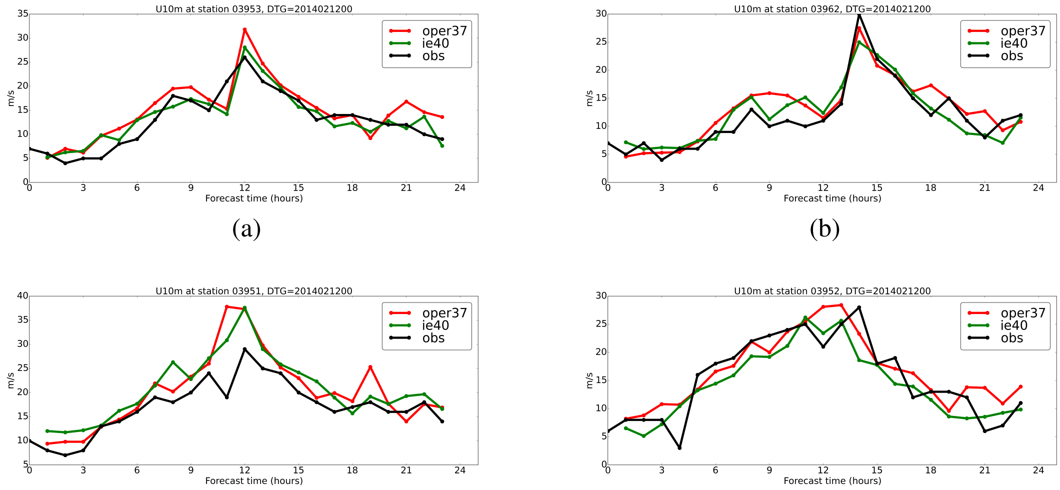

(a) (b) (c) (d)

Figure 28: Forecasted and observed 10 m wind-speeds on the 12$^{\text{th}}$ of February 2014, when Storm Darwin hit Ireland. The forecasts are from the 0000 UTC run on the 12$^{\text{th}}$. Stations shown are (a) Valentia, (b) Shannon Airport, (c) Sherkin Island, and (d) Roches Point.

B.2 Thawing: 25$^{\text{th}}$ of December 2010

During the extremely cold winter in December 2010, very low temperatures on Christmas Day around Dublin began to rise dramatically into the 26$^{\text{th}}$.

Fig. 29 shows 2 m temperature forecasts from the 0000 UTC run on the 25$^{\text{th}}$. Stations shown are Dublin Airport (Fig. 29a) and Casement Aerodrome (Fig. 29b). The oper37 set-up clearly struggles with the extremely low temperatures. The new ie40, while not in any way perfect, manages to capture the general behaviour of the warming much more successfully.

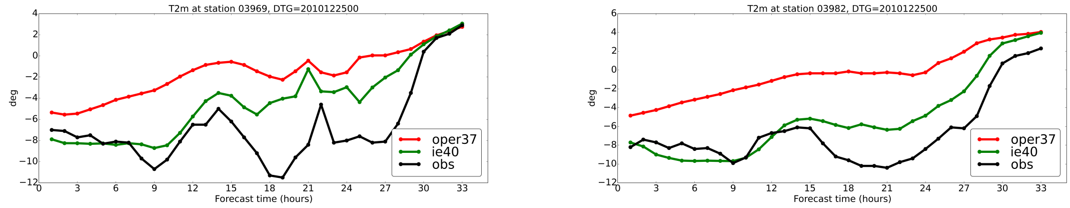

(a) (b)

Figure 29: Forecasted and observed 2 m temperatures on the 25$^{\text{th}}$ of December 2010. The forecasts are from the 0000 UTC run on the 25$^{\text{th}}$. Stations shown are (a) Dublin Airport, and (b) Casement Aerodrome.

B.3 Rain: 8$^{\text{th}}$ of April 2018

On the 8$^{\text{th}}$ of April 2018, heavy showers occurred in some Munster counties. Radar imagery at 1000 UTC is shown in Fig. 30a. Instantaneous rainfall forecasts for this time from the 0000 UTC and 0600 UTC forecast are shown for oper37 (Fig. 30b) and ie40 (Fig. 30c).

It is a known feature of convection-permitting models such as HARMONIE-AROME that the first few hours of forecast time are unreliable for precipitation. In this case, however, even at a lead time of just 4 hours, ie40 is reasonable in predicting the organised system, especially when compared with oper37; compare Fig. 30c with 30b. As well as model changes, a large factor in this improvement is probably the extra cycling (i.e. the three-hour forecast at 0300 UTC) in the new set-up for ie40.

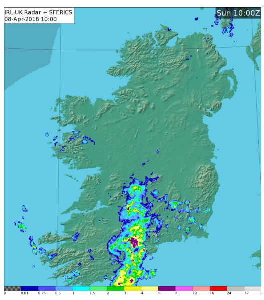

(a)

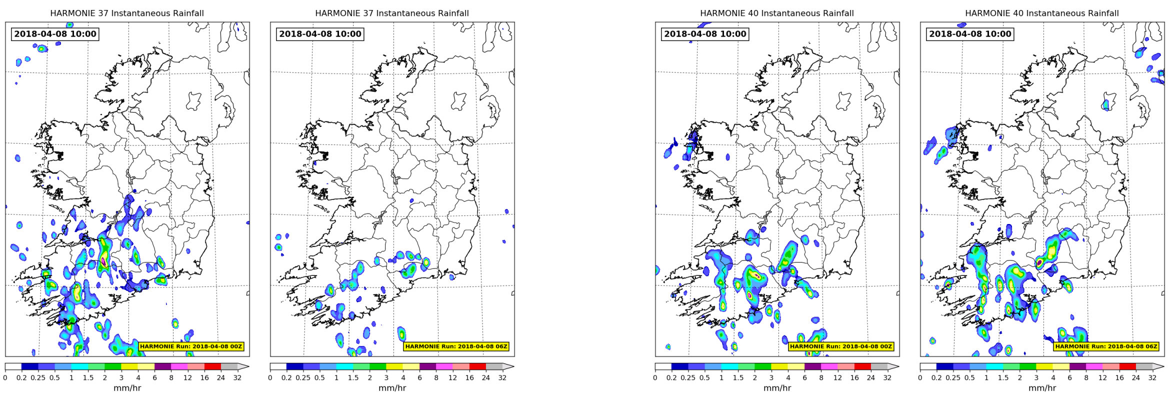

(b) (c)

Figure 30: (a) Radar from 1000 UTC on the 8$^{\text{th}}$ of April 2018. (b) cycle 37h1.1 forecasts of instantaneous rainfall for this time from 0000 UTC (left) and 0600 UTC (right) of the 8$^{\text{th}}$. (c) Similar, for cycle 40h1.1.

B.4 Visibility: 9$^{\mathrm{th}}$ of April 2018

A case of a poor forecast for visibility on the afternoon of the 9$^{\mathrm{th}}$ of April 2018 was reported by forecasters. Satellite images are shown for 1600 UTC, 1700 UTC and 1800 UTC in Figs. 31a, 31b and 31c, respectively, showing a westward progression of low cloud over the Irish Sea. However, forecasts from the operational model at the time showed an essentially static block of low visibility in the area throughout this period (Figs. 31d, 31e and 31f).

Corresponding forecasts from ie40 are shown in Figs. 31g, 31h and 31i. They appear to give a more detailed guidance, capturing the westward progression of the low cloud.

B.5 Fog/visibility: 25$^{\mathrm{th}}$ of March 2018

Here we have another reported case of poor visibility forecasts. In Figs. 32a and 32b the visible and infra-red satellite images for 0900 UTC on the morning of the 25$^{\mathrm{th}}$ of March 2018 show mostly clear conditions over Ireland. The operational forecasts for that time from the 0000 UTC (Fig. 32c) and 0600 UTC (Fig. 32d) forecasts show an over-prediction of fog/low visibility, particularly over the midlands.

In this case, cycle 40h1.1 does not fare better (Figs. 32e and 32f). There is much over-prediction in the east, while the observed band stretching roughly from Limerick to Waterford is missed entirely.

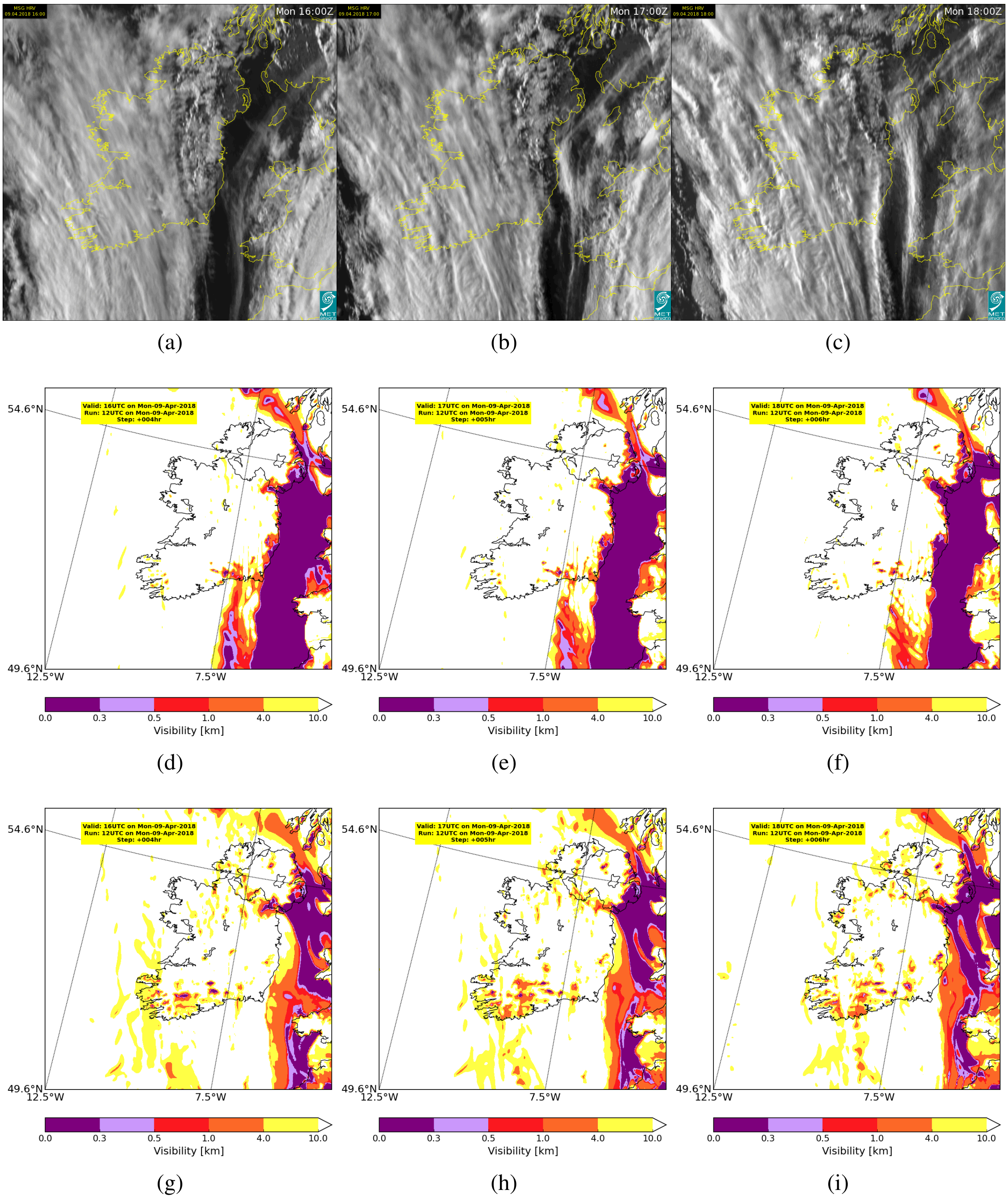

Figure 31: (a)-(c) Visible satellite images for the 1600-1800 UTC on the 29$^{\text{th}}$ of April 2018. Visibility forecasts for these hours are shown for (d)-(f) operational cycle 37h1.1, and (g)-(h) new cycle 40h1.1. In all cases, the forecasts are from the 12UTC run on the 29$^{\text{th}}$.

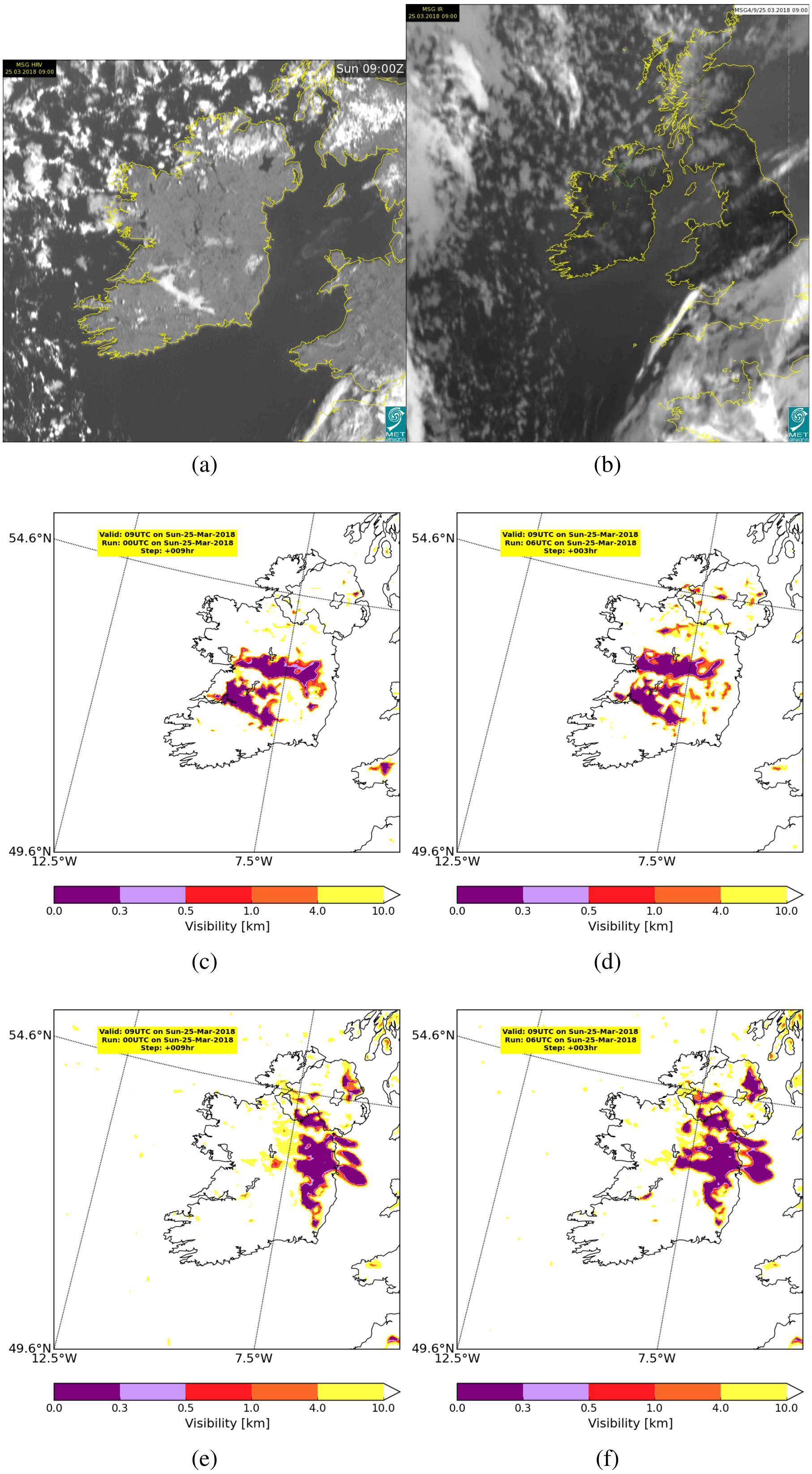

Figure 32: Visible (a) and IR (b) satellite images for 0900 UTC on the 25th of March 2018. Visibility forecasts for this time from the 0000 UTC and 0600 UTC cycles from operational 37h1.1, (c) and (d), and new 40, (e) and (f).